

**The role of the proto-oncogene Ski in cortical
development**

Inauguraldissertation

zur

Erlangung der Würde eines Doktors der Philosophie

Vorgelegt der

Philosophisch-Naturwissenschaftlichen Fakultät

Der Universität Basel

Von

Constanze Katharina Charlotte Baranek

Aus München

Basel 2013

Genehmigt von der Philosophisch-Naturwissenschaftlichen
Fakultät

Auf Antrag von:

Prof. Dr Yves Alain Barde

Prof. Dr Lukas Sommer

Prof. Dr Suzana Atanasoski

Basel, den 24. April 2012

Prof. Dr Martin Spiess

Dekan

Für meinen Vater

(1931-2006)

Table of contents

1	SUMMARY	1
2	INTRODUCTION	2
2.1	DEVELOPMENT OF THE NEOCORTEX	2
2.1.1	THE NEUROEPITHELIUM	2
2.1.2	RADIAL GLIA CELLS	3
2.1.3	INTERMEDIATE PROGENITOR CELLS	4
2.1.4	THE CORTICAL PLATE AND PROJECTION NEURONS	5
2.1.5	AXONAL TARGETS	6
2.1.6	GENETIC MARKERS OF THE CP	7
2.2	THE PROTO-ONCOGENE SKI	9
2.2.1	THE STRUCTURE OF SKI	9
2.2.2	SKI INTERACTION PARTNERS	10
2.2.3	SKI IN DEVELOPMENT	11
2.3	AIM OF THIS THESIS	12
3	RESULTS	13
3.2	SKI PROTEIN IS EXPRESSED IN SUBSETS OF NEURAL PROGENITOR CELLS	14
3.3	SKI PROTEIN IS EXPRESSED IN PROJECTION NEURONS	15
3.4	SKI ABLATION AFFECTS DIFFERENTIATION OF NEURAL PROGENITOR CELLS	17
3.5	THE TIMING OF DEEP-LAYER NEURON GENERATION IS ABERRANT IN SKI MUTANT MICE	19
3.6	INTERMEDIATE PROGENITORS SUBSTITUTE FOR THE LACK OF EARLY BORN NEURONS	20
3.7	SKI IS REQUIRED FOR MAINTAINING THE IDENTITY OF CALLOSAL NEURONS	21
3.8	UL NEURONS ARE BORN AT EXPECTED TIME-POINTS IN SKI DEFICIENT MICE	23
3.9	THE GENETIC PROGRAM OF CP NEURONS IS PARTLY ALTERED IN THE ABSENCE OF SKI	25
3.10	CALLOSAL PROJECTION NEURONS FAIL TO CROSS THE MIDLINE IN SKI MUTANTS	27
3.11	LACK OF SKI IN SATB2-POSITIVE CALLOSAL PROJECTION NEURONS CAUSES THEM TO PROJECT ECTOPICALLY TO SUBCORTICAL TARGETS	29
3.12	SKI INTERACTS WITH SATB2	31
3.13	SKI BINDS WITH SATB2 TO REGULATORY REGIONS OF CTIP2 IN CORTICAL NEURONS	33
3.14	SKI IS PART OF THE NURD COMPLEX WHICH DOWN-REGULATES CTIP2	33

3.15	SKI RECRUITS HDAC1 TO THE NURD COMPLEX	35
4	DISCUSSION	38
4.2	SPATIO-TEMPORAL EXPRESSION PATTERN OF SKI	38
4.3	DOES SKI FUNCTION INDEPENDENTLY IN DIFFERENT COMPARTMENTS?	39
4.4	THE ROLE OF SKI IN INTERMEDIATE PROGENITORS AND MIGRATION	39
4.5	SKI INTERACTS WITH SATB2 IN A TRANSCRIPTIONAL COMPLEX	41
4.6	SKI BINDS WITH SATB2 TO SPECIFIC REGULATORY REGIONS OF CTIP2 IN CORTICAL NEURONS	42
4.7	DOES SKI ACT CELL AUTONOMOUSLY IN CALLOSAL PROJECTION NEURONS?	42
4.8	CONCLUDING REMARKS	44
5	MATERIAL AND METHODS	45
5.2	MICE	45
5.3	IMMUNOHISTOCHEMISTRY, MICROSCOPY AND IMAGE ANALYSIS	45
5.4	BRDU BIRTHDATING	47
5.5	<i>IN SITU</i> HYBRIDIZATION ON TISSUE SECTIONS	48
5.6	PREPARATION OF <i>IN SITU</i> HYBRIDIZATION PROBES	49
5.7	AXONAL TRACING	50
5.8	TRANSIENT TRANSFECTION OF HEK CELLS	51
5.9	CHROMATIN IMMUNOPRECIPITATION (CHIP), COIMMUNOPRECIPITATION (CO-IP), AND IMMUNOBLOTTING	51
5.10	PROXIMITY LIGATION ASSAY (PLA)	52
5.11	LUCIFERASE ASSAY	53
5.12	DATA ANALYSIS	53
6	REFERENCES	54
7	ACKNOWLEDGEMENTS	64
8	CURRICULUM VITAE	65

1 Summary

The proto-oncogene Ski is an evolutionary conserved protein associated with various cellular processes such as proliferation and differentiation as well as transformation and tumor progression. Ski has been found to interact with various factors such as transcription factors, hormone receptors and different members of transcriptional repressor complexes. Since all these results were obtained in cell lines under overexpression conditions, it is not known yet which interactions Ski is involved under physiological conditions.

Ski deficient mice show diverse developmental defects and are perinatal lethal. Even though recent progress has been made in identifying layer and subtype specific genes in the developing cortical plate, little is actually known about their function. In the present work, the endogenous protein Ski is shown to be a new fundamental factor in callosal neuron specification during brain development. In the absence of Ski, misspecified callosal projection neurons largely fail to form the corpus callosum and project instead to subcortical targets.

Ski interacts with the chromatin-remodelling factor Satb2 for transcriptional repression of the transcription factor Ctip2. Neither an interaction with Satb2 nor the regulation of Ctip2 by Ski has been reported yet. Here, for the first time an association of Ski with the NURD complex is shown. A proliferation defect and precocious differentiation in the early brain of Ski deficient mice are described. An altered proliferation of the intermediate progenitor population and a timing defect in neurogenesis of deep layer neurons of the cortical plate are also reported.

These findings demonstrate a central role for Ski in regulating transcriptional mechanisms of callosal neuron specification. They are of particular relevance in view of the essential role of accurate connectivity and identity of neuronal projections.

2 Introduction

2.1 Development of the neocortex

During the development of the mammalian cortex (from embryonic day 11 (E11) to E19 in the mouse), neuronal progenitors located in the ventricular and subventricular zones (VZ /SVZ) of the dorsal telencephalon give rise to multiple projection neurons. These projection neurons are arranged in six cortical layers in the mature brain. Neurons of each layer are generated at similar times and share similar morphologies and patterns of connectivity. During neurogenesis, deep layer neurons (5 and 6) are generated first, followed by neurons of layers 4, 3 and 2.

2.1.1 The neuroepithelium

After closure of the neural tube and before neurogenesis, the developing cerebral cortex is composed of a single sheet of neuroepithelium consisting of a homogenous population of neuroepithelial / neural stem cells. These primary neural progenitors are the origin from which all central nervous system (CNS) neurons will derive (Huttner and Brand, 1997; Gotz and Huttner, 2005; Kriegstein et al., 2006). The cells first proliferate symmetrically to generate two identical daughter cells to set up a progenitor pool of sufficient size. When the pool is extended enough the cells change certain epithelial features and switch to asymmetric, self-renewing divisions to generate one daughter cell and a more specified progenitor such as a radial glia cell, an intermediate progenitor cell or a neuron (Fig. 1.1A and B) (Rakic, 1995; McConnell, 1995; Gotz and Huttner, 2005). Neuroepithelial cells show typical epithelial features, have a prominent apico-basal polarity and show interkinetic nuclear movement (INM) during the cell cycle. The INM gives the neuroepithelium a pseudostratified appearance by an up and down movement of the nucleus through the whole epithelium during the cell cycle. The nucleus locates on the apical side of the ventricle in M-Phase, moves up towards the

basal side of the ventricle during G1, stays there for S-phase and moves back to the apical side during G2. Because of the localization at the apical side of the ventricle during M-phase, these cells are also called apical progenitors (Fig. 1.2A). With the appearance of radial glia cells and asymmetric divisions the neuroepithelium is then called the VZ (Gotz and Huttner, 2005)

A) Symmetric proliferative B) Asymmetric proliferative C) Symmetric differentiative

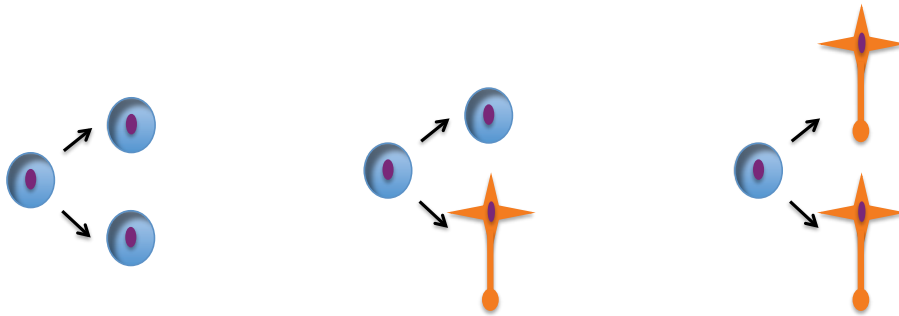


Fig.2.1 Modes of cell division.

Neural progenitor cells divide in an A) symmetric proliferative, B) asymmetric or C) symmetric differentiative way.

2.1.2 Radial glia cells

Radial glia cells (RGCs) represent more fate-restricted progenitors than neuroepithelial cells. They maintain the prominent apico-basal polarity and also undergo interkinetic nuclear migration, but their nucleus remains restricted to the VZ (Fig 2.2B) (Gotz and Huttner, 2005; Malatesta et al., 2008).

RGCs express as neuroepithelium cells Sox2 but also additional markers such as nestin and the antigens recognized by the antibodies RC1 and RC2 as well as typical glial molecules like Blbp, Glast, vimentin and S100beta. RGCs give rise to most of the pyramidal neurons in the cortex but at later time points they are also able to generate oligodendrocytes and astrocytes. It has been shown that the majority of RGCs are committed very early to either neural or glial fates and only a small proportion give rise to both (Malatesta et al., 2008). The transition of neuroepithelial to radial glial cells and their

progression from proliferative to neurogenic divisions during embryogenesis is associated with an increase in the length of their cell cycle (Gotz and Huttner, 2005). Specifically a lengthening of the G1-phase promotes the switch to neurogenesis. Therefore it is hypothesised that an extrinsic or intrinsic cell fate determinant might induce a cell fate change if it is allowed to function for a sufficient length of time (Calegari and Huttner, 2003).

Early in neurogenesis, the majority of neurons arise directly from RGCs by asymmetric division to produce one postmitotic neuron (Haubensak et al.). These neurons migrate radially to the pial surface and form the preplate (PP), a transient neuronal layer which soon gets split in the more superficial marginal zone (MZ) and the deeply located subplate (SP). In between these two layers the cortical plate (CP) develops, forming first deep layers 5 and 6 (Fig. 2.3) (Parnavelas and Nadarajah, 2001).

2.1.3 Intermediate progenitor cells

During middle and late neurogenesis (from E12.5 on) the majority of neurons arise indirectly from RGCs via basally located intermediate progenitor cells (IPCs) (Haubensak et al.; Miyata, 2004; Noctor et al., 2004). IPCs, also called basal progenitors, populate the SVZ divide symmetrically at the basal side of the VZ and produce either only neurons (Fig. 2.1C and Fig. 2.2C) or, in amplifying divisions, pairs of new IPCs. Their main function is to transiently amplify the production of projection neurons from neuroepithelium and RG cells and divide only 1-3 times before neuronal differentiation (Kriegstein et al., 2006). The different progenitor types of apical and basal progenitors can be distinguished as described before either on the basis of their location during M-phase or also by specific markers. Sox2 and pax6 are only expressed in progenitors that divide at the apical surface whereas Tbr2, Svet1 or Cux2 are exclusively expressed in basal progenitors (Englund, 2005; Haubensak et al.; Gotz et al., 1998; Nieto et al., 2004; Tarabykin et al., 2001).

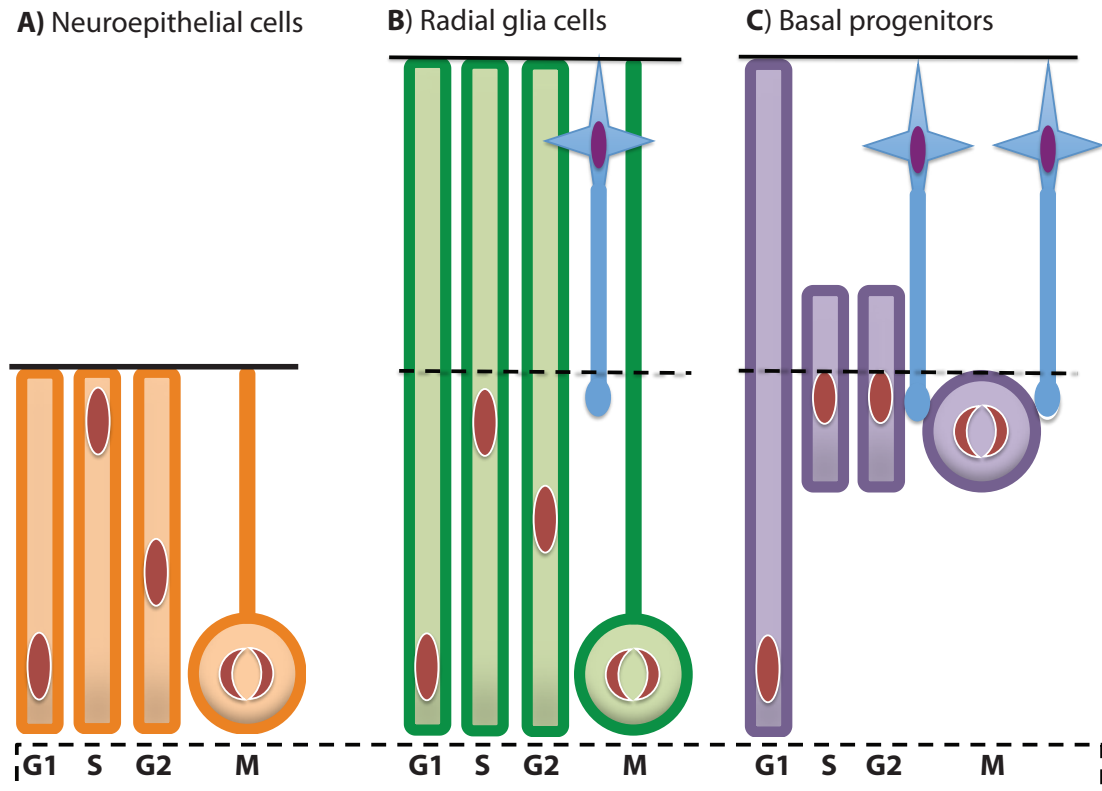


Fig.2.2 Different Progenitor Cells build the neocortex.

A) Neuroepithelial cells span the entire neuroepithelium and show INM throughout the whole apical-basal axis of the cell. B) Radial glia cells maintain the apico-basal polarity of the neuroepithelium and span the whole cortex but their nucleus stays in the VZ. C) Radial glia cells give rise to intermediate progenitors, which divide symmetrically at the basal side of the VZ.

2.1.4 The cortical plate and projection neurons

After specification of the cortical progenitor domains VZ and SVZ (around E12.5 in the dorsal telencephalon) and splitting of the PP, the excitatory projection neurons are generated during approximately the next 6 days. These projection neurons consecutively migrate to their final position within specific layers (Fig 2.3).

The six different layers of the CP are generated in a temporal order and in an inside out manner. Deep layer 6 and 5 neurons are born first (E10.5 – E13.5). Neurons of the superficial layers 4 and 2/3 are born later (E14.5 – E16.5) (Molyneaux et al., 2007). Therefore later born neurons migrate radially to their

final location by passing through the layers of those earlier born neurons (Britanova et al., 2006; Rakic, 2003; Noctor et al., 2001).

Even though the cells which are born at the same time end up in the same layers, the layers themselves are still heterogeneous and contain many different subtypes of projection neurons. These neurons can be classified either according to their specific axonal targets or by genetic markers (Molyneaux et al., 2007; Nelson et al., 2006; Molnár and Cheung, 2006)

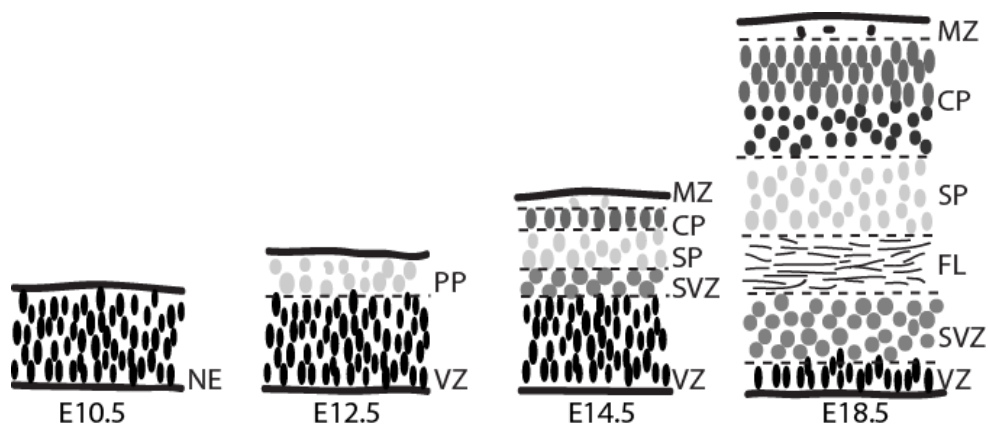


Fig.2.3 Schematic illustration of the cortical wall during cortical development E10.5–E18.5.

NE: neuroepithelium; VZ: Ventricular Zone; SVZ: subventricular zone; PP: preplate; CP: cortical plate; FL: fiber layer; SP: subplate; MZ marginal zone.

2.1.5 Axonal targets

Three basic classes of cortical projection neurons (PNs) are described within the neocortex in reference to their specific projection targets: associative, commissural and cortifugal PNs. Associative PNs extend their axons within the ipsilateral cerebral hemisphere and thus connect only within the same hemisphere. Commissural PN connect to the opposite hemisphere by way of the corpus callosum (CC) or the anterior commissure. Among commissural neurons, the callosal projection neurons (CPN), form a broad and anatomically diverse population of PN. CPNs are located in layers 2/3, 5 and 6. All CPNs extend axons through the CC but can be further defined by their collateral projections. Either they project ipsi- and contralateral to the striatum,

or ipsilateral to the frontal cortex. They never project to targets outside the telencephalon.

Corticofugal PNs project out of the cortex to subcortical or subcerebral targets. Corticofugal PNs are located prevalingly in deep cortical layers 5 and 6 and include corticothalamic, corticotectal, corticopontine and corticospinal neurons (Fig. 2.4) (Molyneaux et al., 2007; Arlotta et al., 2005; Britanova et al., 2005).

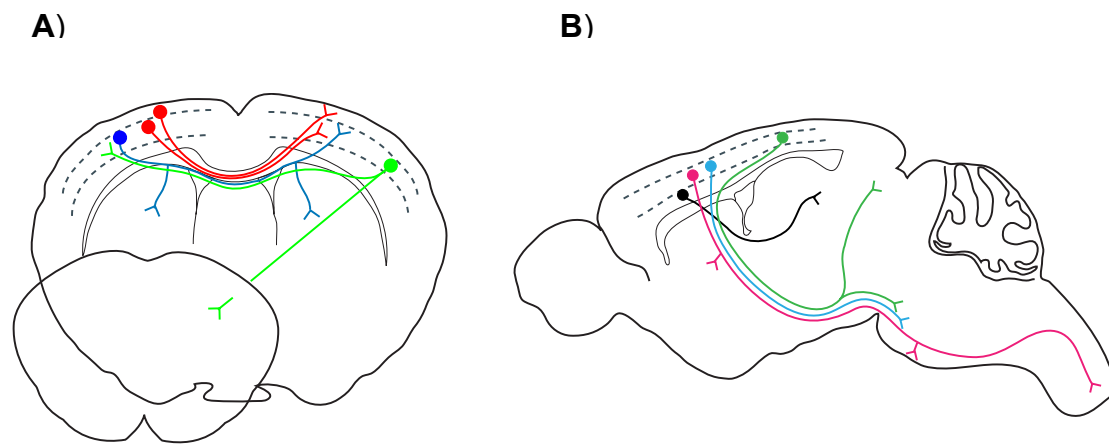


Fig.2.4 Major subtypes of projection neurons within the neocortex .

A) Commissural projections (coronal view): callosal neurons (red), callosal neurons with striatal projections (blue), callosal neurons with ipsilateral frontal projections. B) corticofugal projections (sagittal view): corticothalamic neurons (black), corticotectal neurons (green), corticopontine neurons (blue), corticospinal motor neurons (pink).

2.1.6 Genetic markers of the CP

The number of known layer and subtype specific genes that have been identified in the cortical plate has expanded dramatically in recent years. Several markers have been identified so far for all six layers and their specific subpopulations but in most cases the function of these markers as well as their mechanism of action remain unclear. Examples include among many others: Cux1 (Layer 2/3), Satb2 (layer 2-4), Ctip2 (layer 5) and Tbr1 (layer 6). Until today layer 5 projection neurons are the best studied.

It has been shown for example that loss of Satb2 (special AT-rich sequence binding protein2) leads to ectopic overexpression of Ctip2 in callosally projecting layer 2/3 neurons and induces corticospinally directed growth to the thalamus and the pons. On the other hand loss of Ctip2 (COUP-TF interacting protein 2) causes a malformed capsule and corticofugal axons then do not project past the pons (Britanova et al., 2008a; Alcamo et al., 2008). For Cux1 and its family member Cux2, it has been shown that both regulate dendritic branching, spine development and synapse formation specifically in layer 2/3 (Cubelos et al., 2010). Loss of Sox5, a marker for corticofugal PNs, results in the premature adoption of subcerebral projection neuron features that are characteristic of later stages (Lai et al., 2008). The Tbr1 mutant mouse shows similar defects. These animals exhibit ectopic axon projections to the hypothalamus and the cerebral peduncle and it has been shown that Tbr1 regulates laminar identity in part by downstream activation of Sox5 (Bedogni et al., 2010).

2.2 The proto-oncogene SKI

The proto oncogene Ski was discovered in 1986 as the viral proto-oncogene v-Ski from the avian Sloan-Kettering retroviruses and the v-Ski protein induces the oncogenic transformation of chicken embryo fibroblasts (Li et al., 1986; Stavnezer et al., 1986). It later emerged that the v-Ski protein is a truncated version of the chicken cellular homologue c-Ski (Stavnezer et al., 1989). Several orthologs have been identified in many other species, for example in humans (Nomura et al., 1989), mouse (Lyons et al., 1994), *Xenopus* (Amaravadi et al., 1997) and *Drosophila* (Barrio et al., 2007).

2.2.1 The structure of Ski

C-Ski is a nuclear protein with a size of 727 amino acids (aa) that contains several conserved domains. Two of these are, the Dachshund homology domain (Kim et al., 2002) and a SAND-like domain (Wu et al., 2002), in the N-terminal half and a third domain is a coiled coil domain in the C-terminal region (Nagase et al., 1993). The Dachshund homology domain is a 112 aa long compact globular structure formed out of alpha helix and beta-sheets (Wilson et al., 2004) and defines the Ski gene family with the six members Ski, SnoN, Dach, Fussel-15, Fussel-18 and Corl {Bonnon:2012ho}. The SAND domain (Sp100, AIRE1, NucP41/75 and DEAF) is 95 aa long and forms protein interactions via an extended interaction loop (I-loop) (Fig 2.5). It is found in a number of nuclear proteins which are involved in chromatin-dependent transcriptional regulation. The I-loop of the SAND domain is also responsible for DNA binding. Ski lacks specific DNA binding, and it is suggested that it rather has a regulatory function via protein-protein interactions with co-factors, and thereby modulates transcription (Wu et al., 2002). The coiled coil domain in the C-terminal half contains a tandem repeat and a leucin zipper-like motif, which supports homodimerization as well as heterodimerization with the family member SnoN (Cohen et al., 1999; Heyman and Stavnezer, 1994; Nagase et al., 1993; Sleeman and Laskey, 1993; Zheng et al., 1997).

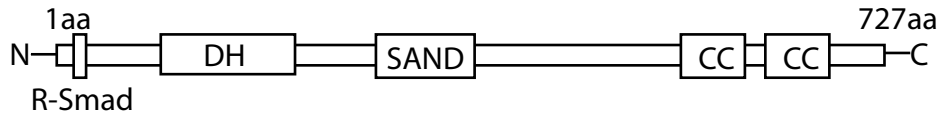


Fig.2.5 Schematic representation of mouse c-ski.

The Ski protein consists out of 727aa and exhibits several conserved domains. DH (Dachshund homology domain), SAND (Sp-100, AIRE1, NucP41/75 and DEAF1), CC (coiled coil domain), R-Smad (Smad binding domain).

2.2.2 Ski interaction partners

In 1999, several groups described Ski as a novel component of the TGF- β signalling pathway. Ski acts as an inhibitor of the TGF- β pathway by association with Smad proteins in response to the activation of TGF- β signalling (Akiyoshi et al., 1999; Luo et al., 1999; Sun et al., 1999; Xu et al., 2000). As an ubiquitously secreted cytokine, TGF- β is known to be involved in a variety of biological processes such as the immune response, but as well as in growth inhibition, differentiation, and induction of apoptosis in various cell types and tissues (Kulkarni et al., 2002).

Other cellular partners of Ski generally fall into two major categories. The first group includes members of the transcriptional repressor complex. Ski can interact with N-CoR (nuclear receptor co-repressor), silencing mediator of retinoid and thyroid hormone receptors (SMRT) and members of HDAC complexes to mediate transcriptional repression of several proteins (Karagianni and Wong, 2007; Nomura et al., 1999; Ueki and Hayman, 2003). In transfected cells it has also been reported that Ski interacts with Sin3A, a general co-repressor involved in HDAC complex recruitment (Nomura et al., 1999). Ski also interacts directly with methyl-CpG-binding protein MeCP2 (Kokura et al., 2001), glioblastoma proteins Gli (Dai et al., 2002) and recently it has been shown that Ski is additionally part of protein complexes of p53 histon deacetylase SIRT1 (Inoue et al., 2011).

The second group of Ski-binding partners includes molecules involved in differentiation, proliferation or hormonal responses: Ski has been shown to interact with RAR alpha to block its transactivation activity (Dahl et al., 1998) and with vitamin D receptor to repress vitamin D signalling (Ueki and Hayman,

2003). Ski blocks the DNA binding activity of GATA1 (Ueki et al., 2004), binds to members of the nuclear factor family (NFI) (Tarapore et al., 1997) and also to the transcription factors c-Jun (Pessah et al., 2002) and PU.1 (Ueki et al., 2008). Through its interaction with pRb, Ski abrogates Rb-mediated transcriptional repression (Tokitou et al., 1999). It also attenuates the function of an other tumour suppressor, p53 (Inoue et al., 2011).

2.2.3 Ski in development

Widespread *in vivo* investigations in *Xenopus*, zebrafish and mice revealed critical roles for Ski during development. Sleeman and Laskey showed in 1993 in *Xenopus* oocytes the presence of c-Ski transcripts during early development and their maternal regulation. Later an important role for Ski in embryonic development was suggested, when it was shown that overexpression of c-Ski RNA in *Xenopus* explants led to secondary formal axis formation and neuron-specific gene expression (Amaravadi et al., 1997). The ability of Ski to induce neural cell fate requires its ability to interact with BMP-specific Smads and to repress them (Wang et al., 2000). The study of Kaufman et al in 2000 in Zebrafish suggested first a role of c-Ski in neural patterning, after they showed that overexpression of SkiA and SkiB leads to a disruption of gastrulation and to a dorsalized phenotype (Kaufman et al., 2000).

In mice, c-Ski transcripts are found in almost all adult tissues at relatively low levels. The same is found during embryogenesis with the highest expression in brain and lung. However, in embryogenesis an increase of Ski expression at E8.5 to E9.5 in the neural tube and migrating neural crest cells (Lyons et al., 1994) and from E12.5 to E15.5 in skeletal muscle has been described (Colmenares and Stavnezer, 1995). The phenotype of the Ski-knockout mouse generated in the group of C. Colmenares confirmed that c-Ski plays a role in neural patterning and muscle differentiation (Berk et al., 1997). Ski-deficient mice are perinatal lethal and have a strong reduction in skeletal muscle mass (Berk et al., 1997), a finding which is consistent with the

observation of skeletal muscle hypertrophy of type II skeletal muscle fibers in mice overexpressing c-ski (Sutrave et al., 1990).

Ski deficient mice also show strong neural defects such as an exencephaly due to a failure in cranial neural tube closure. The severity of this phenotype is strain dependent. In the genetic C57BL6/J background a facial clefting appears instead. Additionally, Atanasoski et al. could show in the peripheral nervous system Ski expression in Schwann cells *in vivo* and its regulatory function on myelin related genes (Atanasoski et al., 2004). In all strains, skeletal abnormalities as well as digit and eye defects have been described (Berk et al., 1997; Colmenares et al., 2002)

The 1p36 syndrome in human includes deficiencies related to those found in the Ski knock-out mouse, suggesting that the phenotype might depend to some extent on the depletion of *Ski* on chromosome 1p36.3 (Colmenares et al., 2002; Rosenfeld et al., 2010).

2.3 Aim of this thesis

The aim of this thesis is to characterise the role of Ski in cortical development. Spatio-temporal and co-expression studies of the Ski protein together with different markers will be used to identify the brain regions in which Ski is expressed and exerts its function. By comparison of wildtype and Ski knock-out brains, defects caused by the loss of Ski will be described. Further potential interactions of markers co-expressed with Ski will be tested and the role of Ski in these interaction analysed.

3 RESULTS

The protooncogene Ski cooperates with the chromatin-remodeling factor Satb2 in specifying callosal neurons

Constanze Baranek¹, Manuela Dittrich¹, Srinivas Parthasarathy², Carine Gaiser Bonnon^{1,3}, Olga Britanova², Clemencia Colmenares⁴, Victor Tarabykin², and Suzana Atanasoski^{1,3}

¹Institute of Physiology, Department of Biomedicine, University of Basel, CH-4056 Basel

²Institute of Cell Biology and Neurobiology, NeuroCure Cluster of Excellence, Charité–Universitätsmedizin Berlin, Campus Mitte, D-10117 Berlin

³Institute of Anatomy and Cell Biology, Albert-Ludwigs-University Freiburg, D-79104 Freiburg

⁴Department of Cancer Biology, Lerner Research Institute, Cleveland, Ohio 44195

The following chapter is based on the work published in Proceedings of the National Academy of Science of the United States (PNAS), February 2012, Volume 109, issue 9, pages 3546-3551.

3.2 Ski protein is expressed in subsets of neural progenitor cells

We first analysed Ski protein expression by immunohistochemistry, and found that it was expressed throughout the neuroepithelium at E10.5 (Fig. 3.1A), where it co-localized with neural stem cell markers (Fig. 3.1B and C). The specificity of the anti-Ski antibody was demonstrated by the lack of signal on E10.5 *Ski*^{-/-} sections (Fig. 3.1D). Ski expression was maintained in the ventricular zone (VZ) of the telencephalon at E12.5 (Fig. 3.1E). Notably, Ski was down regulated in *Tbr2*-positive intermediate progenitor cells in the subventricular zone (SVZ), and was absent from the earliest-born *HuC/D*-positive neurons, which form the preplate (PP) (Fig. 3.1F and G).

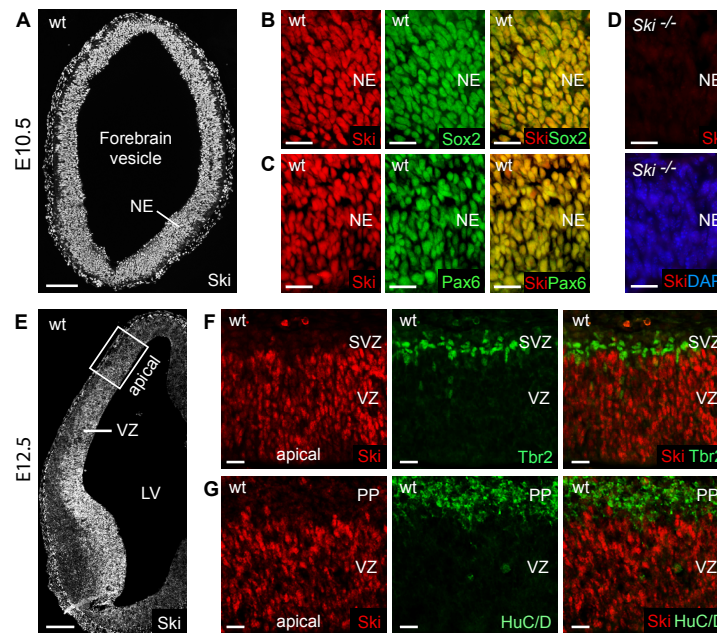


Fig. 3.1. Expression of Ski in wild type (wt) neural progenitor cells of the forebrain.

(A) Ski immunohistochemistry on horizontal forebrain sections at E10.5 reveals prominent Ski expression throughout the neuroepithelium (NE). (B,C) Higher magnifications of the NE show costaining of Ski and Sox2 (B), and Ski and Pax6 (C) in nuclei of neuroepithelial/radial glia cells (yellow in the corresponding overlays). (D) Ski signal is absent in DAPI-stained nuclei (blue) on E10.5 horizontal forebrain sections of *Ski*^{-/-} mice, demonstrating the specificity of the anti-Ski antibody. (E) On coronal brain sections at E12.5, Ski protein is detected in the VZ of the telencephalon in a ventral-to-dorsal gradient. (F,G) High-magnification images from the dorsal telencephalon at E12.5 (boxed region in E) show double immunostainings for Ski and *Tbr2* (F) and Ski and *HuC/D* (G). Note that in the overlays Ski is absent from *Tbr2*-positive intermediate cells in the SVZ (E) and from

early-born, HuC/D-positive neurons forming the preplate (PP) (F). Bars: A,E, 100 μm ; B–D,F–G, 20 μm . LV, lateral ventricle.

3.3 Ski protein is expressed in projection neurons

Ski continued to display strong expression in the VZ at E14.5 (Fig. 3.2A, left panel). In addition, it appeared in postmitotic cells of the developing cortical plate (CP) at E14.5, and was strongly expressed in the dorso-medial part of the rostral telencephalon at E17.5 (Fig. 3.2A, right panel). Higher-magnification images demonstrate that most Ski-positive cells reside in superficial layers of the CP, with a distribution similar to that of the Satb2-expressing population (Fig. 3.2B). A smaller number of Ski-positive cells was present in layer V and even fewer in layer VI, layers that are defined by immunoreactivity for Ctip2 and Tbr1, respectively (Fig. 3.2B). To characterize the subpopulation of Ski-expressing neurons, we performed double immunostainings for Ski and a panel of layer-specific markers, including Satb2, Ctip2, and Tbr1 (Fig. 3.2C–F). At E17.5, Satb2 is expressed in callosal projection neurons in upper layers, as well as in subsets of DL neurons that comprise a diverse population of callosal and subcortical projection neurons (Britanova et al., 2008a). On the other hand, Ctip2 and Tbr1 are expressed in different subsets of DL neurons that project to subcortical targets. We find that subpopulations of Ski-positive neurons express Satb2 in superficial layers of the CP (approx. 85%) and in deep layers V and VI (approx. 30%) (Fig. 3.2C). Conversely, the majority of Satb2-positive cells coexpressed Ski in upper layers, although many Satb2-positive cells in deep layers were Ski-negative (Fig. 3.2C). In addition, virtually all layer V neurons expressing high levels of Ctip2 were positive for Ski (Fig. 3.2D). Notably, very few cells were triple positive for Ski, Satb2, and Ctip2 (Fig. 3.2E, arrow), which is in agreement with previous findings demonstrating that less than 5% of Satb2-positive cells express Ctip2 in deep layers (Alcamo et al., 2008). Little coexpression was observed for Ski and Tbr1 at E17.5 (Fig. 3.2F). The dynamic expression pattern of Ski points to a temporally restricted and cell-type specific function of Ski in cortical cells.

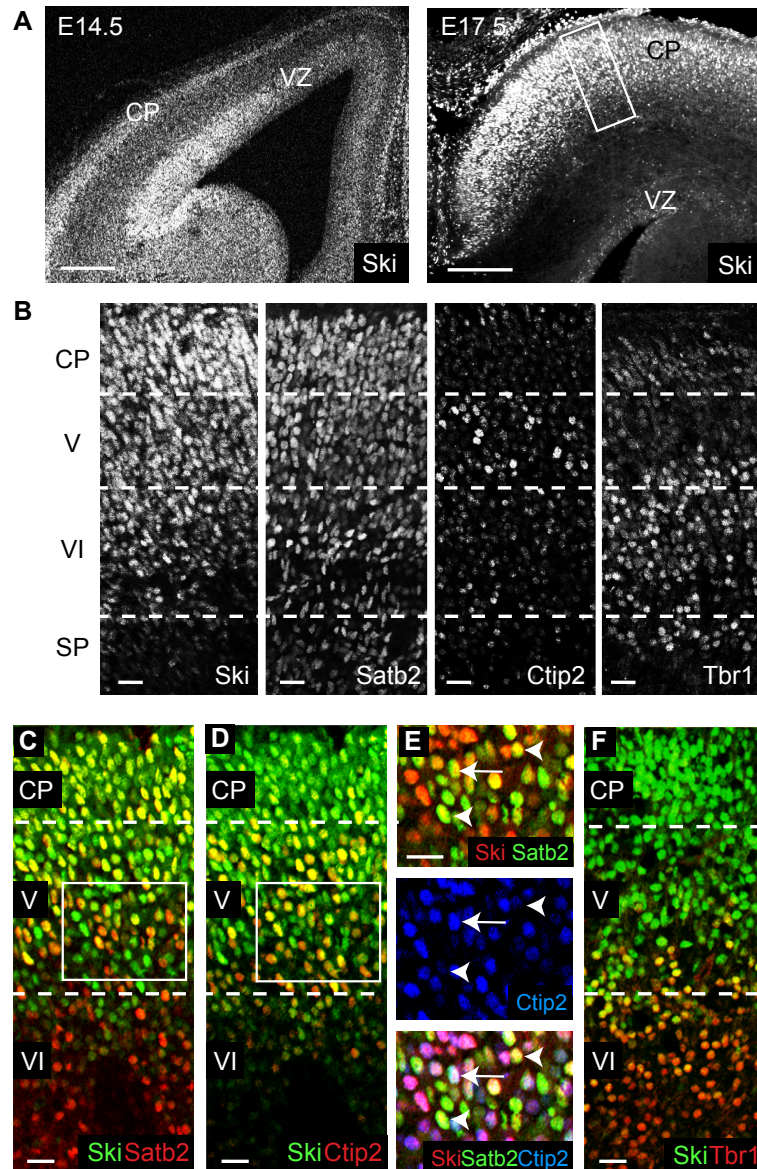


Fig. 3.2. Ski is expressed in postmitotic cells of the developing neocortex.

(A) Ski immunostaining on coronal brain sections is predominantly detected in the VZ of the dorsal and ventral telencephalon, and in postmitotic cells of the neocortex at E14.5 and E17.5 (A). (B) Higher-magnification images of the rostro-dorsal neocortex at E17.5 (boxed region in A, right panel) show that neurons expressing high levels of Ski are mainly located in the superficial layers of the cortical plate (CP) and in layer V as visualized by layer-specific markers Satb2, Ctip2 and Tbr1. (C,D) Ski shows high coexpression with Satb2 in upper layers of the CP and to a minor extent in layer V (yellow in the corresponding overlays) (C), and with Ctip2 in layer V neurons (D). (E) Triple immunostainings for Ski, Satb2, and Ctip2 in higher-magnification images (boxed region in C,D) show that most Ski and Satb2 double positive cells (yellow in upper panel, arrow and arrowheads) do not express Ctip2 (blue in middle panel, arrowheads). A rare triple-positive cell is depicted (white in lower panel, arrow). (F) Ski and Tbr1 are coexpressed to a minor extent in layer VI neurons. Bars: A, 200 μ m; B–F, 20 μ m.

3.4 Ski ablation affects differentiation of neural progenitor cells

We used Ski^{-/-} mice (Berk et al., 1997) to investigate the requirement for Ski during cortical development. Analysis of the dorsal telencephalon at E10.5 revealed a reduction in radial neuroepithelial thickness in Ski^{-/-} forebrains compared to wild type (wt) (wt: 101±10µm; Ski^{-/-}: 74±2µm, n=6, P ≤ 0.001) (Fig. 3.3A). Moreover, immunostainings for the M-phase marker phospho-histone H3 (pHH3) (Fig. 3.3A) showed fewer proliferating apical progenitor cells in mutant forebrains (Fig. 3.3B). Similarly, the pool of intermediate progenitors was also affected in Ski^{-/-} embryos (Fig. 3.3E and F). Concomitantly, we observed increased numbers of cells positive for doublecortin (Dcx; marker of migrating postmitotic neurons) in Ski^{-/-} versus wt forebrains (Fig. 3.3C and D). Thus, our findings suggest that as a result of Ski deletion, cells differentiate precociously into neurons, leading to a reduced progenitor pool at initial stages of corticogenesis.

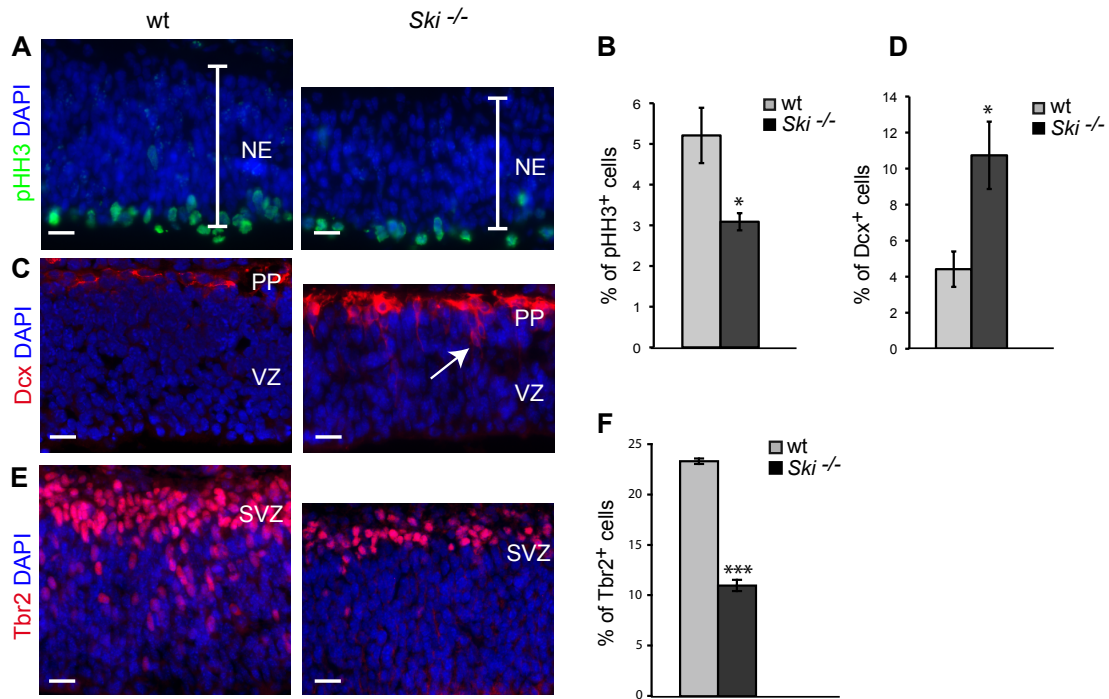


Fig. 3.3. Ski ablation reduces neural progenitor cell numbers and causes premature neurogenesis in the dorsal telencephalon.

(A) Immunostaining for phospho-histone H3 (pHH3), a marker for cells in M phase, and DAPI staining of horizontal E10.5 wt and *Ski*^{-/-} forebrain sections. Fewer mitotically active apical progenitor cells are present in *Ski*^{-/-}, and radial thickness of the mutant neuroepithelium (NE) is reduced (white bars in A). (B) Numbers of pHH3-positive cells in wt and *Ski*^{-/-} are expressed as percentage of total DAPI stained nuclei per field. (C) Immunostaining for doublecortin (Dcx), a marker of immature neurons, reveals increased neurogenesis in E10.5 *Ski*^{-/-} forebrain. In wt, Dcx-positive cells are present in the preplate (PP), while in *Ski*^{-/-}, Dcx-expressing neurons are additionally detected within the VZ (arrow in C, right panel). (D) Numbers of Dcx-positive cells in wt and *Ski*^{-/-} are expressed as percentage of total DAPI stained nuclei per field. (E) Immunofluorescence for Tbr2 on coronal sections of E12.5 dorsal telencephalon shows a substantial decrease in the number of intermediate progenitor cells in *Ski*^{-/-}. (F) Numbers of Tbr2-positive nuclei in wt and *Ski*^{-/-} are expressed as percentage of total DAPI stained nuclei per field. Bars: 20 μ m. Data are the mean of at least three embryos per genotype. Error bars indicate s.e.m. Student's t-test: (*) $P \leq 0.05$, (***) $P \leq 0.001$.

Despite this defect, *Ski*^{-/-} brains revealed only a slight reduction of forebrain size at E17.5, and DAPI-stained coronal sections showed only a moderate reduction of cortical thickness compared to wt (Fig. 3.4A and B).

3.5 The timing of deep-layer neuron generation is aberrant in *Ski* mutant mice

To further investigate the timing of neuronal generation, pregnant females were injected with BrdU at E10.5, E12.5, or E14.5 to label proliferating cells, and the total number of pulse-labeled progeny was assessed at E17.5 (Fig. 3.4C and D). The percentage of total BrdU-positive neurons generated at E10.5 and E12.5 was lower in *Ski*^{-/-} (Fig. 3.4D), presumably because of the decreased pool of progenitor cells at these time-points (Fig. 3.3B and E). However, we found an excess number of neurons born at E14.5 in the mutant (Fig. 3.4D).

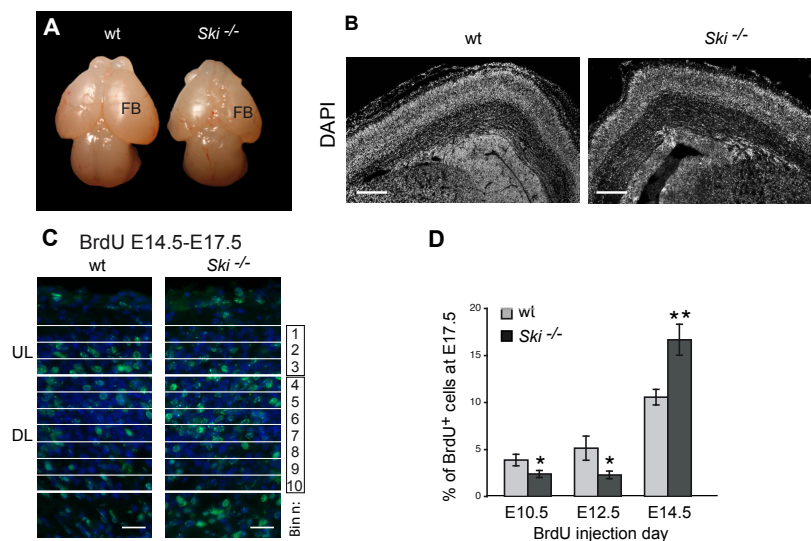


Fig. 3.4. Corticogenesis is impaired in the *Ski*^{-/-} neocortex.

(A) Dorsal views of wt and mutant brains reveal a slight reduction of forebrain size (FB) in *Ski*^{-/-} mice. (B) DAPI staining of coronal sections through E18.5 cortices shows that the thickness of the cerebral wall is slightly reduced in mutant mice. (C) Photomicrographs of neocortical sections show the representative distribution of E14.5 BrdU birth date-labeled cells in wt and *Ski*^{-/-}. For the quantification of labeled cells the cortical thickness was divided into ten equal bins. The bold white lines indicate the boundaries between the upper layers of the cortical plate (UL, bins 1–3), and deep layers (DL, bins 7–10). (D) Quantification of BrdU-labeled cells in E17.5 neocortices after single BrdU injections at E10.5, E12.5, or E14.5 is shown. The graphical summary of the results represents the overall number of neurons generated at E10.5, E12.5, and E14.5, respectively, in wt and *Ski*^{-/-}. Bars: B, 200 μ m; C, 20 μ m. Data are the mean of at least three embryos per genotype. Error bars indicate s.e.m. Student's t-test: (*) $P \leq 0.05$, (**) $P \leq 0.01$.

3.6 Intermediate progenitors substitute for the lack of early born neurons

At the same time, the number of proliferating intermediate progenitors was increased in *Ski*^{-/-} versus wt (Fig. 3.5A,B, and D) and the pool of Tbr2-positive progenitors was comparable between genotypes by E14.5 (Fig. 3.5C). Thus, during mid-corticogenesis, intermediate progenitors are likely to substitute for the lack of sufficient numbers of progenitors during early corticogenesis, ultimately leading to comparable thickness and cell numbers in corresponding wt and mutant cortical layers at E17.5 (Fig. 3.4B).

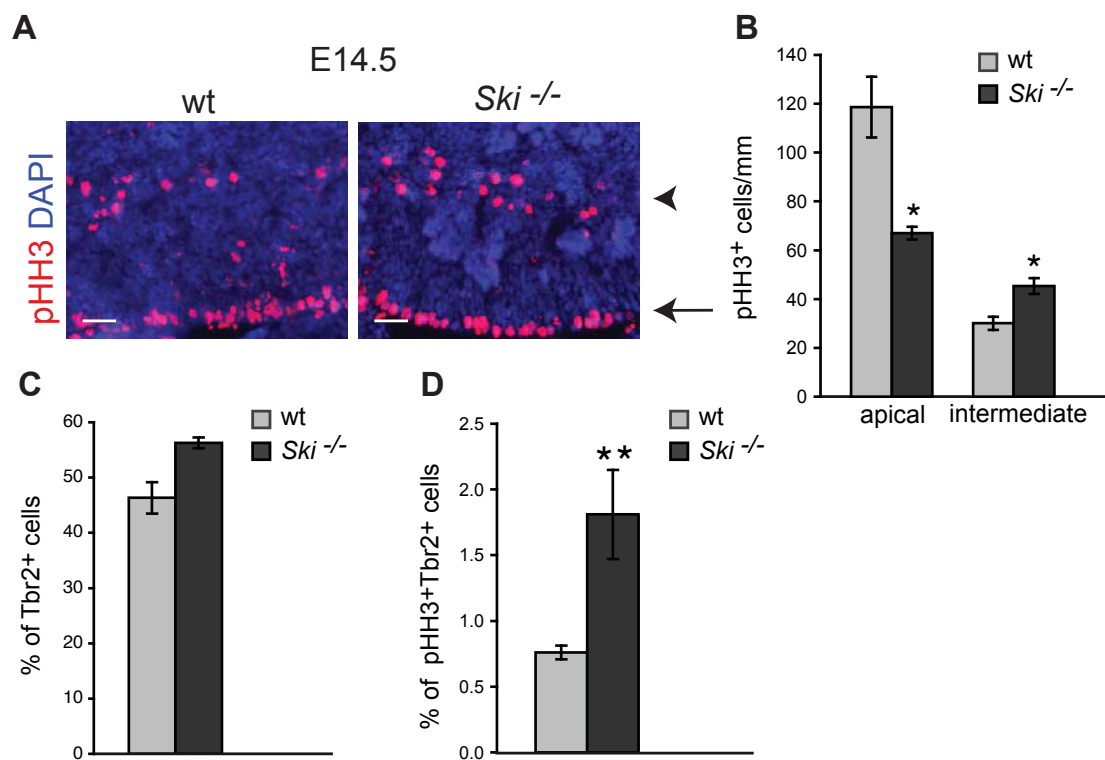


Fig. 3.5. Proliferation of apical and intermediate progenitors is disturbed in *Ski* mutants at E14.5.

(A) Immunostaining for M phase marker pHH3 and DAPI staining of horizontal E14.5 wt and *Ski*^{-/-} forebrain sections reveals fewer apical (arrow), but more intermediate mitotically active progenitor cells (arrowhead) in *Ski*^{-/-} compared to wt. (B) Quantification of the number of pHH3-positive cells per ventricular surface length (mm) in wt and *Ski*^{-/-}. (C) Numbers of Tbr2-positive nuclei in wt and *Ski*^{-/-} are expressed as percentage of total DAPI stained nuclei per field. (D) Numbers of proliferating pHH3-positive intermediate (Tbr2⁺) progenitors in wt and *Ski*^{-/-} are expressed as percentage of total Tbr2 stained nuclei per field. Bar: 20 μ m. Data are

the mean of at least three embryos per genotype. Error bars indicate s.e.m. Student's t-test: (*) $P \leq 0.05$, (**) $P \leq 0.01$.

3.7 Ski is required for maintaining the identity of callosal neurons

We next examined neuronal identities in mutant cortices. For this, we assessed and compared the distribution of cell-type specific markers by immunohistochemistry at E17.5 in the neocortex of wt and mutant (Fig. 3.6). *Satb2* was expressed normally in all layers (CP, V, VI, SP) in the absence of *Ski* (Fig. 3.6A). In contrast, in *Ski*^{-/-} mutants expression of *Ctip2*, a marker for cortico-subcortical projection neurons, was markedly expanded to the superficial layers of the CP, where *Ctip2* is normally absent (Fig. 3.6B). Further, the number of cells expressing *Tbr1* in the UL neurons was reduced in *Ski*-deficient embryos, whereas *Tbr1* expression in layer VI and in the subplate remained unchanged (Fig. 3.6C). To further characterize cells expressing *Ctip2* ectopically, coronal sections were double-stained for *Satb2* and *Ctip2* (Fig. 3.6D and E). In the superficial layers of the CP, *Satb2*-positive cells were negative for the deep layer marker *Ctip2* in the wt (Fig. 3.6D and E) (Alcamo et al., 2008), while in the mutant, most *Satb2*-positive cells ectopically expressed *Ctip2* (Fig. 3.6D and E). In deep layers, approx. 2% (42/2286) of total cells coexpressed *Satb2* and *Ctip2* in the wt (Fig. 3.6D), while in the mutant, the percentage of double-stained cells increased to approx. 7% (166/2444) (Fig. 3.6D and E). Collectively, these results demonstrate that subpopulations of *Satb2*-positive neurons in both upper and deep layers ectopically express *Ctip2* upon loss of *Ski*, but that this effect is more prominent in UL neurons at the examined time-point.

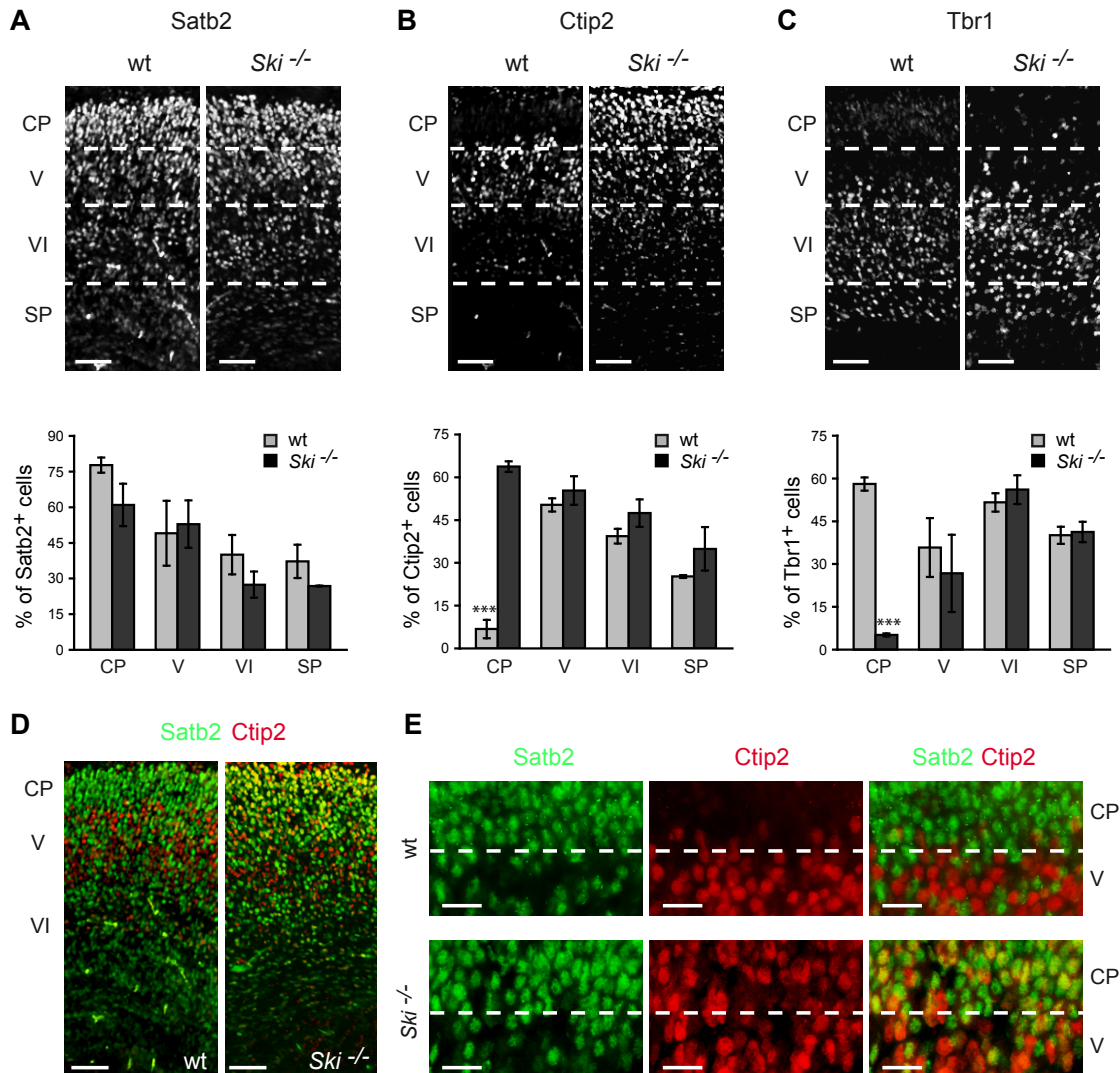


Fig. 3.6. Ski deletion affects Ctip2 and Tbr1 expression patterns in the dorsal telencephalon.

(A-C) Satb2 immunostaining of E17.5 coronal brain sections is similar in wt and *Ski*^{-/-} cortex (A). Ctip2 immunoreactivity has expanded to the superficial layers of the CP in the absence of *Ski* (B), and fewer cells in the upper layers of the CP express Tbr1 in *Ski*^{-/-} mice (C). Quantification of Satb2, Ctip2, and Tbr1-positive neurons is shown for the superficial layers of the CP, the deep layers V and VI, and the subplate (SP) as a percentage of total DAPI stained nuclei per field within the respective layer in wt (grey bars) and *Ski*^{-/-} (black bars). Statistically significant differences were found in the numbers of Ctip2-positive cells (B) and Tbr1-positive cells (C) in the upper layers of the CP. (D,E) Double immunostainings for Satb2 and Ctip2 on E17.5 coronal brain sections in wt and *Ski*^{-/-} (D). Higher-magnification images reveal ectopic expression of Ctip2 (red) in Satb2-positive cells (green) in *Ski* mutants (E, lower panels), while Ctip2 expression is absent in Satb2-positive cells of the wt (E, upper panels). Bars: A-D, 50 μ m; E, 20 μ m. Data are the mean of at least three embryos per genotype. Error bars indicate s.d.

3.8 UL neurons are born at expected time-points in *Ski* deficient mice

To investigate the origin of the *Ctip2* and *Satb2* double-labeled cells in the upper layers, we performed BrdU pulse labeling at E12.5 and E14.5, and determined the distribution of BrdU-positive neurons among those expressing *Ctip2*, *Satb2*, or the specific UL marker *Cux1* (Fig. 3.7A and Fig. 3.7C and D). We find that in contrast to the wt, *Ctip2*-positive cells born at E14.5 reach the upper layers in *Ski*^{-/-} embryos (Fig. 3.7A). Mutant *Ctip2*-positive cells born at E12.5, however, migrate to deep layers as in the wt, and do not aberrantly reach the upper layers by E17.5 (Fig. 3.7A). Further, our results show that the distribution of *Cux1*-positive neurons that were born at E14.5 is similar between genotypes at E17.5, suggesting that UL neurons are generated at the expected time point and migrate to the expected layers in the mutant (Fig. 3.7A). In support of this notion, very low numbers of *Cux1*-positive, UL neurons were born at earlier stages, both in the wt and the *Ski*^{-/-} (Fig. 3.7D). The analysis of *Satb2*-positive neurons born at E14.5 showed a similar distribution in wt and *Ski*^{-/-} (Fig. 3.7A). In summary, UL neurons in the *Ski*^{-/-} mutants are born at the expected time-point, but ectopically express *Ctip2*. In support of this conclusion, we find increased expression of *Ctip2* mRNA in mutant cortices (Fig. 3.7B).

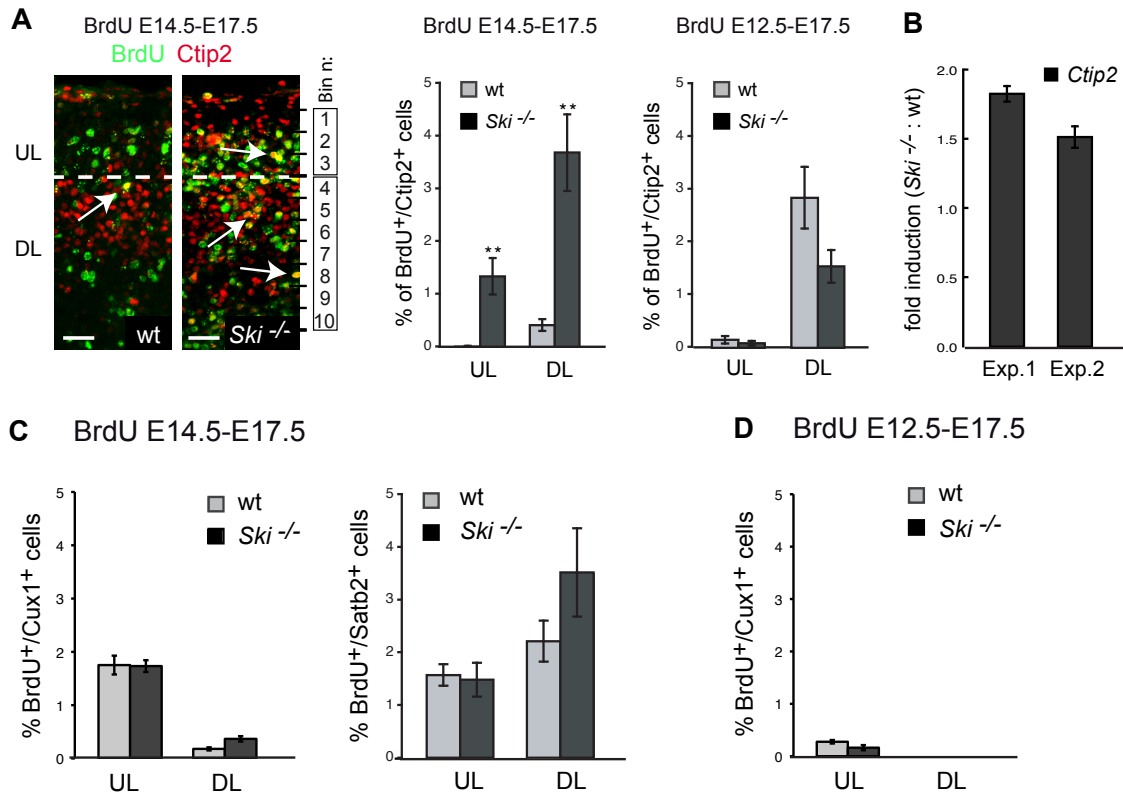


Fig. 3.7. Quantification of BrdU-labeled cells in E17.5 neocortices after single BrdU injections at E12.5 and E14.5.

(A) Photomicrographs of neocortical sections show the representative distribution of E14.5 BrdU birth date-labeled, *Ctip2*-positive cells in wt and *Ski*^{-/-} (arrows). For the quantification of labeled cells the cortical thickness was divided into ten equal bins. Bins 1-3 correspond to the upper layers (UL), and bins 7-10 to the deep layers (DL) of the cortical plate. The percentage of BrdU-labeled cells, double positive for *Ctip2* in each region (UL, DL) relative to the total number of DAPI stained nuclei per field was determined in wt (grey bars) and *Ski*^{-/-} (black bars) (middle and right panels). The analysis shows that the numbers of E14.5-born *Ctip2*-positive cells that populate the UL and DL are significantly increased in the mutant. However, the increase in *Ctip2*-positive cells in the mutant UL is not due to a precocious generation of these cells, as *Ctip2*-positive cells born at E12.5 are predominantly found in the DL in both genotypes. (B) qRT-PCR was performed to determine *Ctip2* mRNA levels in wt and *Ski*^{-/-} cortices at E18.5. *Ctip2* values were normalized to HPRT1 mRNA. cDNA from brains of two wt/*Ski*^{-/-} littermates (Exp.1 and Exp. 2) were generated. Results are presented as ratios of *Ctip2* levels in *Ski*^{-/-} and wt, demonstrating an approx. 1.5 and 1.8-fold induction of *Ctip2* in the *Ski*^{-/-} mutant. (C,D) The percentage of BrdU-labeled cells, double positive for either *Cux1* or *Satb2* in each region (UL, DL) relative to the total number of DAPI stained nuclei per field was determined in wt (grey bars) and *Ski*^{-/-} (black bars). (C) The analysis shows that comparable numbers of E14.5-born cells expressing UL markers *Cux1* or *Satb2* reach the UL. (D) The analysis of *Cux1*-positive cells born at E12.5 underlines the finding that no excess UL neurons are generated at earlier time-points in the mutant. Bar: F, 20 μ m. Data are the mean of at least three embryos per genotype. Error bars indicate s.e.m. in (A-D). Student's t-test: (**) $P \leq 0.01$, (***) $P \leq 0.001$. (B) M.Dittrich

3.9 The genetic program of CP neurons is partly altered in the absence of Ski

These experiments show definitively that subpopulations of Ski-deficient, *Satb2*-positive neurons change their genetic program. To further characterize the phenotype of the mutant callosal neurons, we performed *in situ* hybridization assays including fate- and layer-specific markers (Fig. 3.8A-C) (Alcamo et al., 2008). In addition to *Ctip2*, other corticospinal motor neuron (CSMN)-specific genes, such as *Clim1/Ldb2* and *Cdh13* displayed increased expression levels in deep layers and an expansion of expression into upper layers in E18.5 Ski mutants. However, another CSMN-specific gene, the transcription factor *Fezf2* was expressed normally, suggesting that Ski-deficient callosal neurons acquire some but not all characteristics of wt CSMNs (Fig. 3.8A). Further, the expression of callosal projection neuron (CPN)-specific genes, including the expression of *Cdh10*, *Ptn*, and *Lmo4* was upregulated upon loss of Ski, consistent with a disturbed CPN identity (Fig. 3.8B). We also tested layer-specific genes, and found that *Cux2* was elevated in the intermediate zone, while expression of the transcription factor *bHLHb5* in layers II-V was reduced in the Ski mutant (Fig. 3.8C). However, not all expression patterns of genes were altered. For example, the expression of the signaling molecule *Dkk3*, and the layer-specific markers *Cux1*, *ROR β* , and *Bcl6* remained normal in the absence of Ski (Fig. 3.8B and C). Overall, Ski-deficient callosal neurons display a phenotype which is reminiscent of and partially overlapping with that of *Satb2*-deficient mice, where *Satb2* mutant neurons acquired ectopic expression of *Ctip2* and other CSMN-specific genes, and lost their identity as callosal projection neurons (Britanova et al., 2008a; Alcamo et al., 2008).

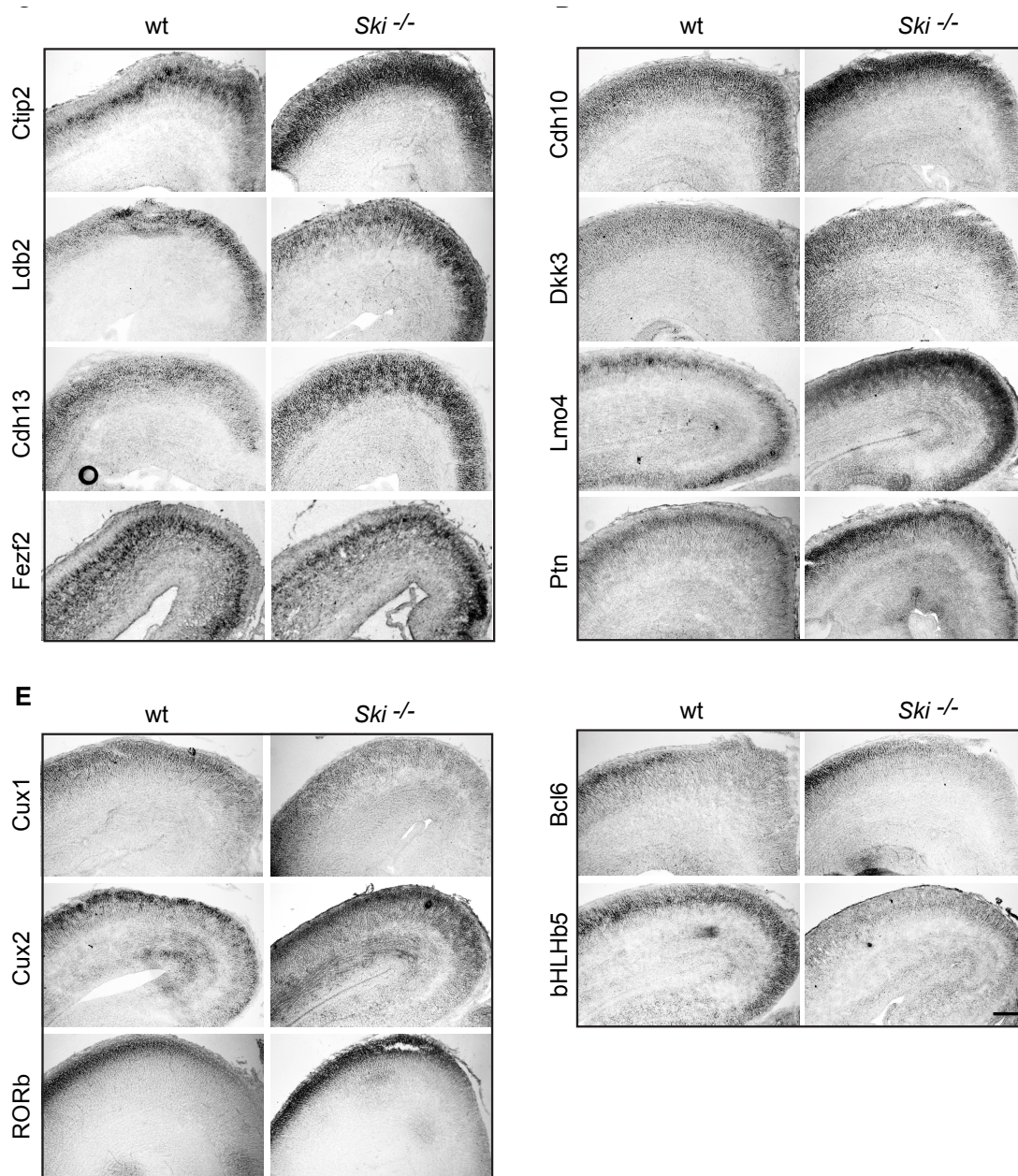


Fig.3.8. Layer-specific markers are differentially expressed in *Ski*^{-/-} cortices.

In situ hybridization reveals that the expression levels of CSMN-specific genes is either elevated (*Ctip2*, *Ldb2*, and *Cdh13*) or normal (*Fezf2*) in the *Ski*^{-/-} mutant (A). Similarly, the expression of CPN-specific genes is either elevated (*Cdh10*, *Lmo4*, and *Ptn*) or normal (*Dkk-3*) relative to the wt expression levels in the cortical plate (B). While the expression of the 2,3,4 layer marker *Cux1* is unchanged, the expression levels of the 2,3,4 layer marker *Cux2* is elevated in the mutant IZ. Further, the expression of 4 and 5 layer marker *RORβ* and the superficial CP marker *Bcl6* is normal, while the expression level of the layer 2–5 marker *bHLHb5* is drastically reduced upon loss of *Ski* (C). Bar: 200 μm for C-E.

3.10 Callosal projection neurons fail to cross the midline in *Ski* mutants

Thus, we next evaluated whether the formation of the corpus callosum was also impaired in the *Ski* mutants (Fig. 3.9). Immunohistochemical staining for the neural cell adhesion molecule L1 revealed striking alterations in axonal connectivity in *Ski* mutants. Axonal tracts either failed to cross the midline, or the population of L1-positive axons forming the corpus callosum was largely decreased (Fig. 3.9A). To investigate the origin of axons arriving at the midline, we performed tract tracing by placing crystals of the lipophilic marker Dil in the neocortex of wt and *Ski*^{-/-} at E18.5, allowing an anterograde labeling of cortical axons traveling to the contralateral hemisphere. Coronal sections of rostral levels showed that in contrast to the wt, Dil-labeled axons in the mutant approached the midline, but did not cross it (Fig. 3.9B). Similarly to the findings in the *Satb2* mutant (Alcamo et al., 2008), the development of the glial sling, which is required for axons to grow contralaterally (Shu et al., 2003), appeared normal in the *Ski* mutant (Fig. 3.9C), suggesting that the malformation of the corpus callosum is not solely based on a midline defect.

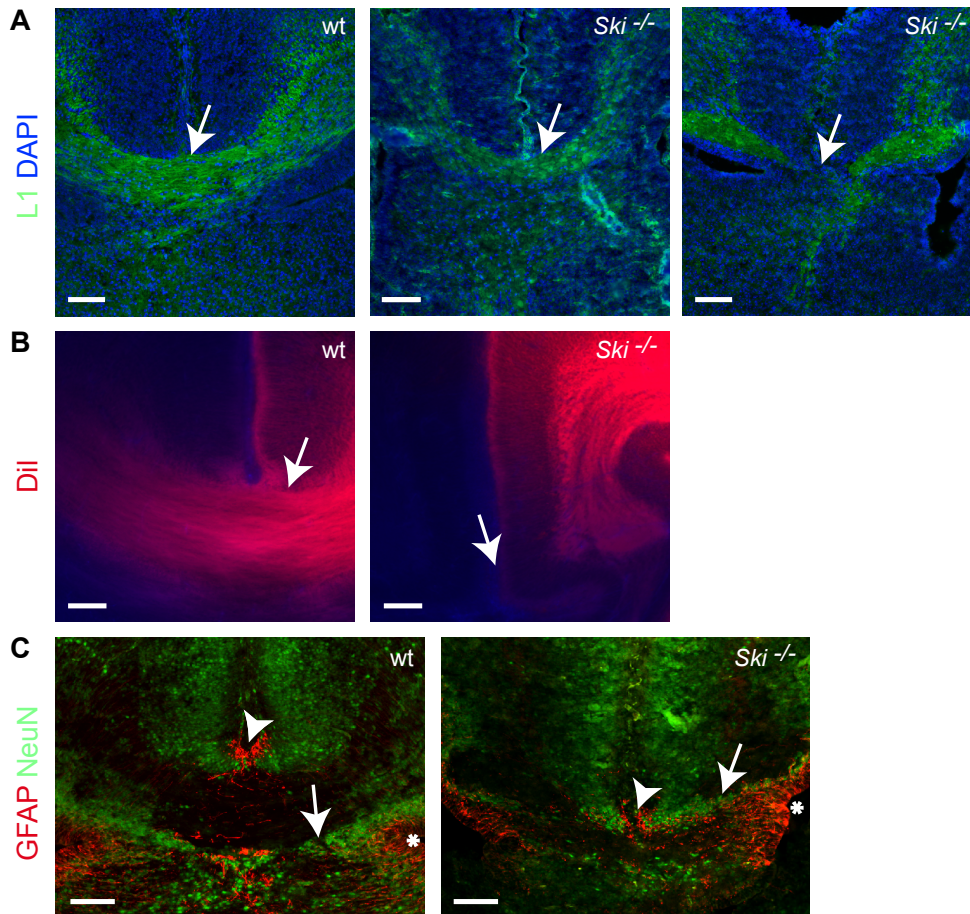


Fig. 3.9. Ski deletion leads to failure in the formation of the corpus callosum.

(A) Immunohistochemistry for the axonal marker L1 on E18.5 coronal brain sections depicts axonal projections forming the corpus callosum. In comparison to wt (arrow in left panel), the population of axons crossing the corpus callosum is largely decreased (arrow in middle panel) or is completely missing (arrow in right panel) in *Ski*^{-/-} embryos. (B) Dil labeling from the neocortex at E18.5 demonstrates that cortical efferent fibers form the corpus callosum in wt, but not in *Ski*^{-/-} embryos (arrows). (C) Double immunohistochemistry for the neuronal marker NeuN and the glial marker GFAP shows the presence of the glial sling (arrow), the glial wedge (asterisk), and the induseum griseum (arrowhead) in wt and *Ski*^{-/-}. Note that these structures are present in *Ski* mutants, but the corpus callosum is missing. Bars: 100 μm

3.11 Lack of Ski in Satb2-positive callosal projection neurons causes them to project ectopically to subcortical targets

We next examined whether axonal projections of Satb2-positive neurons were altered in the absence of Ski. For this, we placed Dil in the cerebral peduncle at E18.5 (Fig. 3.10A and B) to retrogradely label cortico-subcerebral projections (Fig. 3.10C and D). In these experiments, we concentrated on the dorso-medial cortex, and we specifically studied the contribution of Satb2-expressing neurons to cortico-subcerebral projections (Fig. 3.10E). We found that approx. 55% (214/392) of subcerebrally projecting neurons, retrogradely labeled from the cerebral peduncle, were Satb2-positive in wt mice, while the percentage of Dil-positive, Satb2-expressing cells increased to approx. 84% (343/408) in the *Ski* mutant. Thus, the percentage of Satb2-expressing neurons that project via the cerebral peduncle was markedly increased in the *Ski* mutants as compared to the wt (Fig. 3.10F). Taken together, our data show that callosally projecting neurons redirect their axons to subcortical targets in the absence of Ski, as described previously in *Satb2*^{-/-} mutants (Britanova et al., 2008a; Alcamo et al., 2008). These similarities between the *Ski*^{-/-} and *Satb2*^{-/-} phenotypes prompted us to evaluate whether Ski and Satb2 act in a common genetic pathway.

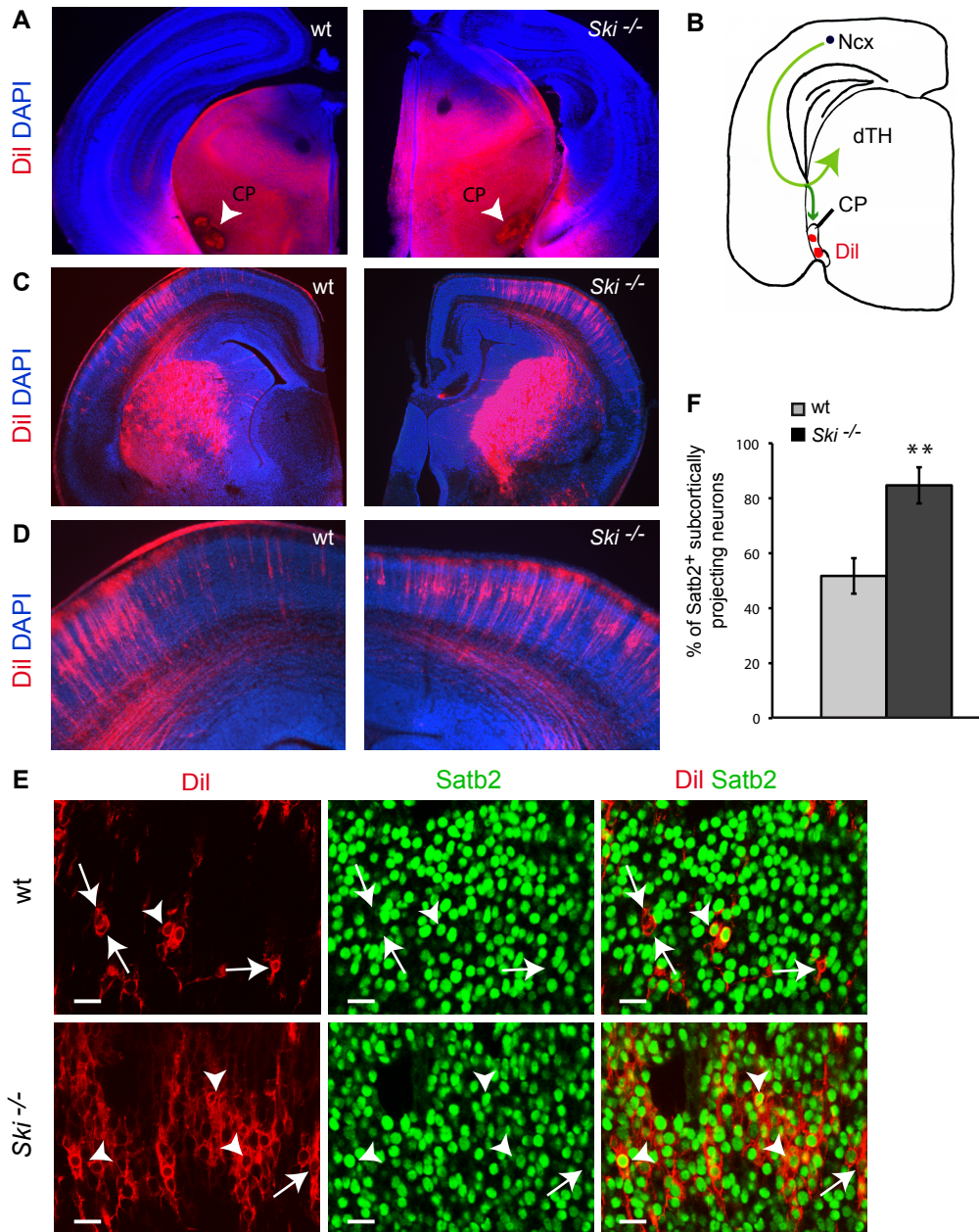


Fig. 3.10. Callosal neurons redirect their axons towards subcortical targets in *Ski* mutants.

(A) The placement of Dil crystals in the cerebral peduncle (CP, arrowheads) in wt and *Ski*^{-/-}. (B) Schematic representation showing the position of Dil crystal placement in the CP. Ncx, neocortex; dTH, dorsal thalamus. (C) Dil placed in the CP retrogradely labels subcerebrally projecting cortical neurons in both wt and *Ski*^{-/-}. (D) Higher-magnifications of wt and *Ski*^{-/-} cortical plate shown in (C). (E,F) Colocalizing the retrogradely labeled neurons with Satb2 shows that the majority of Dil-labeled neurons are Satb2-positive in the *Ski*^{-/-} mutant (arrowheads in E), while more Dil-labeled neurons are Satb2-negative in the wt (arrows in E). The percentage of subcortically projecting neurons that are Satb2-positive is significantly higher in *Ski* mutants as compared to wt (F). Bars: 20 μ m. Error bars indicate s.e.m. Student's t-test: (**) $P \leq 0.01$. The figure was kindly provided by S. Parthasarathy.

3.12 Ski interacts with Satb2

To investigate whether these two factors interact, we cotransfected HEK293 cells with Ski and Satb2 expression vectors and performed immunoprecipitation experiments using lysates of cotransfected and control untransfected cells (Fig. 3.11A and B). Immunoblots with Ski and Satb2-specific antibodies, respectively, showed that Ski and Satb2 coprecipitated (Fig. 3.11A). As no Ski or Satb2 immunoreactivity was detected when using control antibody, this experiment identifies Satb2 as a novel intracellular partner of Ski. These results were confirmed using cortical lysates demonstrating the presence of Ski-Satb2 complex formation *in vivo* (Fig. 3.11B). To examine the location of endogenous Ski and Satb2 complexes in the developing cortex, we applied an antibody-based proximity ligation assay (PLA), which allows individual interacting pairs of protein molecules to be visualized *in situ* (Söderberg et al., 2006) (see Materials and Methods). Specific Ski-Satb2 complex formation was observed in nuclei of UL neurons (Fig. 3.11C, arrows in upper panel), while there was no signal detectable on control *Ski*^{-/-} or *Satb2*^{-/-} sections (Fig. 3.11C, middle and lower panels).

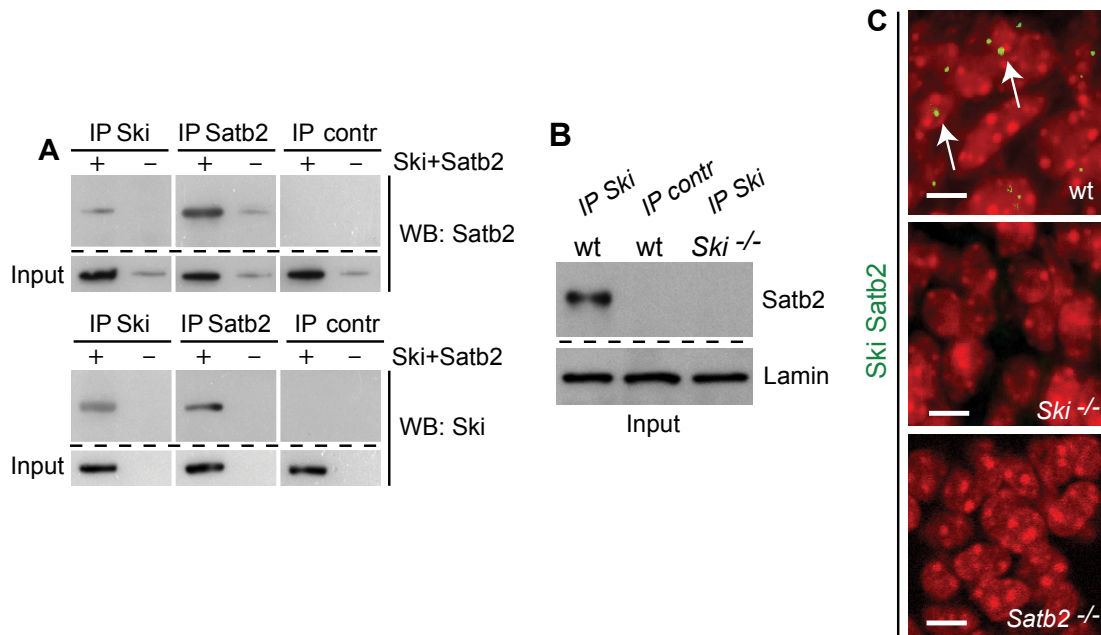


Fig. 3.11. Ski associates with Satb2 and represses *Ctip2* transcription in cortical neurons.

(A) Lysates from Ski and Satb2-cotransfected (+) and untransfected (-) HEK cells were analyzed by immunoprecipitation (IP) with anti-Ski antibody (Ab) (IP Ski), anti-Satb2 Ab (IP Satb2), or an unrelated control Ab (IP contr). Western blotting was subsequently performed using Abs against Satb2 (upper panel) or Ski (lower panel). Note that HEK cells endogenously express low levels of Satb2 (input in upper panel), while there is no endogenous Ski detectable (Input in lower panel). (B) Lysates of wt cortical tissue were analyzed by IP with anti-Ski Ab (IP Ski) or an unrelated control Ab (IP contr) followed by immunoblotting using Abs against Satb2. An IP with anti-Ski Ab (IP Ski) with lysates of *Ski*^{-/-} cortical tissue served as control to demonstrate the specificity of the anti-Ski antibody. Equal input of protein extracts was controlled by Lamin detection. (C) Endogenous Ski-Satb2 complexes were detected *in situ* in cortical neurons on wt brain sections using the proximity ligation assay (PLA). Panels represent magnifications of wt, *Ski*^{-/-}, and *Satb2*^{-/-} superficial layers of the CP. The Duolink fluorescent probe 563 (see Methods) was used as hybridization probe (green) and the nuclei were stained with TO-PRO®-3 stain (red). The Ski-Satb2 complex formation in the wt (arrows in upper panel) was specific, as there was no signal detectable in the *Ski*^{-/-} and *Satb2*^{-/-} (middle and lower panels). Bars: C and H, 5 μ m. Fig. A: M. Dittrich. Fig. B: M. Dittrich/C. Gaiser.

3.13 Ski binds with Satb2 to regulatory regions of *Ctip2* in cortical neurons

We next investigated whether Ski targets regulatory sequences of *Ctip2* (Fig. 3.12). Since Ski does not directly interact with DNA, but interacts with Satb2, we asked whether Ski is recruited to the previously identified Satb2-binding sites in the *Ctip2* gene locus *in vivo* (Alcamo et al., 2008) (Fig. 3.12A). We performed chromatin immunoprecipitation (ChIP) with mouse E18.5/P0 cortical tissue using a Ski antibody and previously published primer pairs for targeting sequences of matrix attachment regions (MARs) within the *Ctip2* locus (amplicons within five *Ctip2* MAR regions: A1-A6) (Alcamo et al., 2008) (Fig. 3.12A). The analysis using cortical lysates revealed an enrichment of five MAR sequences (A1-A5), suggesting that Ski was targeted to complexes at multiple MAR sequences within the *Ctip2* locus (Fig. 3.12D). Since the enrichment of the A4 amplicon was most prominent, we next examined Ski-Satb2 complex formation at this site. Semiquantitative and quantitative PCR with primer pairs amplifying the A4 site disclosed a specific Ski protein/*Ctip2* DNA complex in wt, which was substantially reduced in the absence of Satb2 protein and was undetectable in the *Ski*^{-/-} negative control (Fig. 3.12B and Fig. 3.12E). In contrast, ChIP experiments with Satb2 antibody revealed that Satb2-binding to the A4 site was as efficient in the absence of Ski as in wt (Fig. 3.12B and Fig. 3.12E). Taken together, we demonstrate that in the presence of Satb2, Ski is recruited to the *Ctip2* locus *in vivo*, but Satb2-binding to the *Ctip2* cis-regulatory region is independent of Ski.

3.14 Ski is part of the NURD complex which down-regulates *Ctip2*

As previously reported, Satb2 downregulates *Ctip2* expression by interacting with two members of the NURD complex, the histone deacetylases HDAC1 and MTA2 (Britanova et al., 2008a). Thus, to further evaluate the role of Ski in the formation of repressor complexes on the *Ctip2* gene, we then asked

whether the NURD/Ctip2 DNA complex was affected by *Ski* deletion. ChIP experiments with MTA2 and HDAC1 revealed that only MTA2, but not HDAC1 interacted with the *Ctip2* locus in the absence of *Ski* (Fig. 3.12C and Fig. 3.12E).

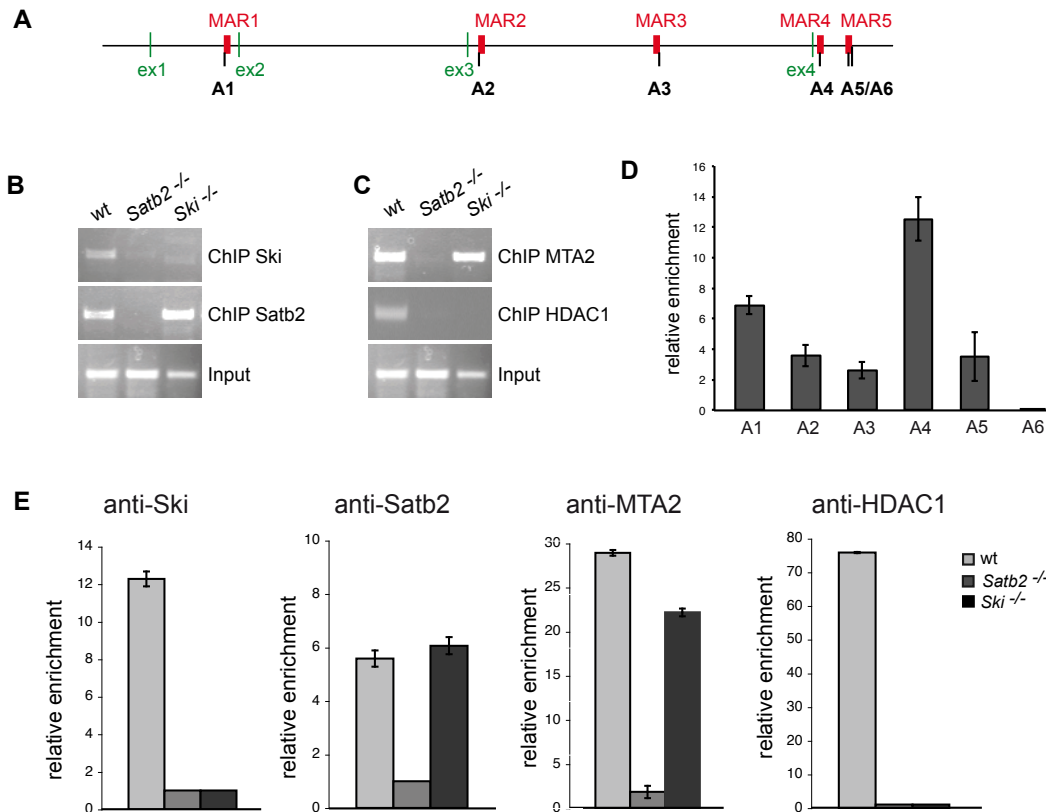


Fig. 3.12. *Ski* is essential for recruiting HDAC1 to the NURD complex.

(A) A schematic representation of the *Ctip2* locus (adapted from Alcamo et al., 2008). Green bars indicate exons 1-4 (ex1-ex4). Matrix attachment regions 1-5 (MAR 1-5) are shown as red bars. ChIP amplicons 1-6 (A1-A6) and their position in the locus are depicted below. (B,C) Semiquantitative chromatin immunoprecipitation (ChIP) assay was performed to detect protein occupancy at the *Ctip2* locus using wt, *Ski*^{-/-}, and *Satb2*^{-/-} cortical tissue from E18.5/P0 pups. A 245 bp fragment was amplified from a previously described *Ctip2* regulatory DNA sequence, the matrix attachment region 4 (Alcamo et al., 2008) (A and E). The samples were immunoprecipitated with anti-*Ski* and anti-*Satb2* antibodies (C), or anti-MTA2 and anti-HDAC1 (D) ChIP assay to detect *Ski* occupancy at the *Ctip2* locus (amplicons A1-A6) using wt cortical tissue from E18.5 pups. (E) ChIP assay to detect protein occupancy at the *Ctip2* locus (amplicon A4) using wt, *Ski*^{-/-}, and *Satb2*^{-/-} cortical tissue from E18.5/P0 pups. The samples were immunoprecipitated with anti-*Ski*, anti-*Satb2*, anti-MTA2, or anti-HDAC1 antibodies. The results are normalized to the levels of the *Ski*^{-/-} sample for ChIPs with anti-*Ski* antibodies, to the levels of the *Satb2*^{-/-} sample for ChIPs with anti-*Satb2* antibodies, and to the levels of a negative antibody control for ChIPs with anti-MTA2 and anti-HDAC1 antibodies. The analysis confirms the results shown in Fig. B and C, and demonstrates that *Satb2* and MTA2 bind to the *Ctip2* locus in the

absence of Ski, but HDAC1 is not recruited to the site. Each bar represents the mean value of three PCR experiments. Error bars indicate s.e.m.

3.15 Ski recruits HDAC1 to the NURD complex

To add further evidence that Ski is required for the recruitment of HDAC1 to the Satb2-containing repressor complex, we performed co-immunoprecipitation studies for Satb2, MTA2, and HDAC1 on cortical cell lysates (Fig. 3.13A and B). Our data demonstrate that Satb2 and MTA2 interactions were largely unaffected in the Ski mutant compared to wt (Fig. 3.13B), while Satb2-HDAC1 complex formation was markedly reduced in the absence of Ski (Fig. 3.13A). Further, *in situ* PLA assays showed that in the absence of Satb2, Ski-MTA2 interactions were reduced compared to wt (Fig. 3.13C, panels to the left), while MTA2-Satb2 interactions were readily found in the absence of Ski (Fig. 3.13C, middle panels), and no Satb2-HDAC1 complexes were detectable upon loss of Ski (Fig. 3.13C, panels to the right). To further assess the role of Ski in transcription of *Ctip2*, we performed transient transfection assays with a *fos-luciferase* reporter containing MAR region A4. As shown in Fig. 3.13D, concomitant expression of Satb2 and Ski in transfected COS cells was necessary to reduce the activity of the A4-*fos-luciferase* reporter approx. 2-fold, whereas no change in activity was detected upon expression of either protein alone.

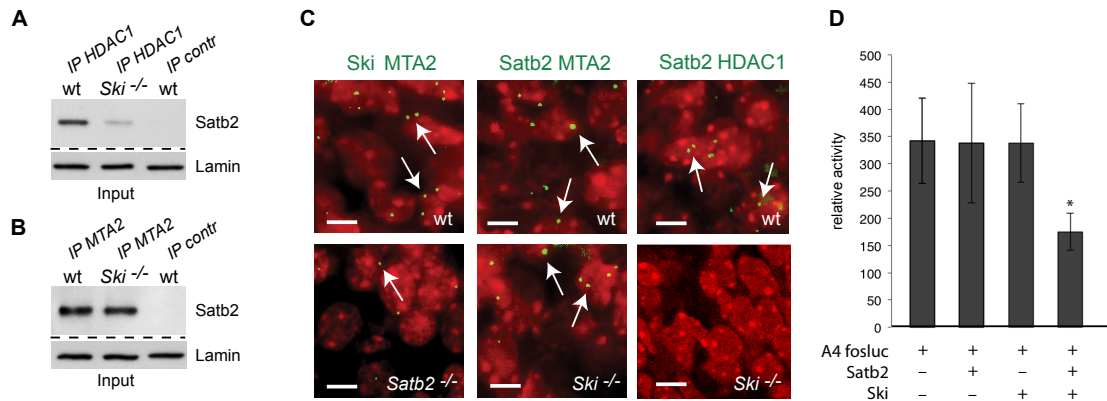


Fig. 3.13. In the absence of Ski or Satb2 is the assembly of the NURD complex disturbed.

(A,B) Lysates of wt and *Ski*^{-/-} cortical tissue were analyzed by IP with anti-HDAC Ab (IP HDAC) (A) or anti-MTA2 Ab (IP MTA2) (B) followed by immunoblotting using Abs against Satb2 (A,B). An unrelated Ab was used as control (IP contr) (A,B). Equal input of protein extracts was controlled by Lamin detection (F,G). Note that Satb2-HDAC complex formation is drastically reduced in the *Ski*^{-/-} (A), while Satb2-MTA2 complex formation is unaffected in the absence of Ski (B). The IP experiments were repeated at least three times (A,B). (C) Using PLA, endogenous protein complex formation was detected in UL neurons *in situ* as indicated on wt, *Ski*^{-/-}, and *Satb2*^{-/-} cortical brain sections (arrows). Note that Satb2-HDAC1 complex formation is absent in UL neurons on *Ski*^{-/-} sections. (D) A4 sequence activity in presence or absence of Satb2 and/or Ski in COS cells transfected with a *fos-luciferase* reporter construct that contains the A4 sequence. Bars: C and H, 5 μ m. FigA/B M.Dittrich and C.Gaiser.Fig.D: O.Britanova.

These results demonstrate that Ski is necessary for the Satb2-mediated A4 transcriptional repression *in vitro*, and further support our *in vivo* finding that both proteins are required to repress *Ctip2* expression. Alcamo et al. (2008) previously demonstrated that forced expression of Satb2 alone led to a substantial decrease of the A4 sequence activity in mouse EL4 lymphoma cells. These cells are likely to express endogenous Ski, as previously reported for numerous cancer cell lines {Bonnon:2012ho}; this may explain the observed cell-type related differences. Taken together, our findings demonstrate that *Ctip2* is a direct target of Ski and Satb2 in cortical neurons, and that both proteins are required for efficient recruitment of members of the NURD complex to the *Ctip2* locus. While Satb2 directly binds MAR sequences in the *Ctip2* locus and recruits MTA2 to the site, Ski is required for attracting HDAC1, thereby allowing the NURD complex to form appropriately (Fig. 3.14).

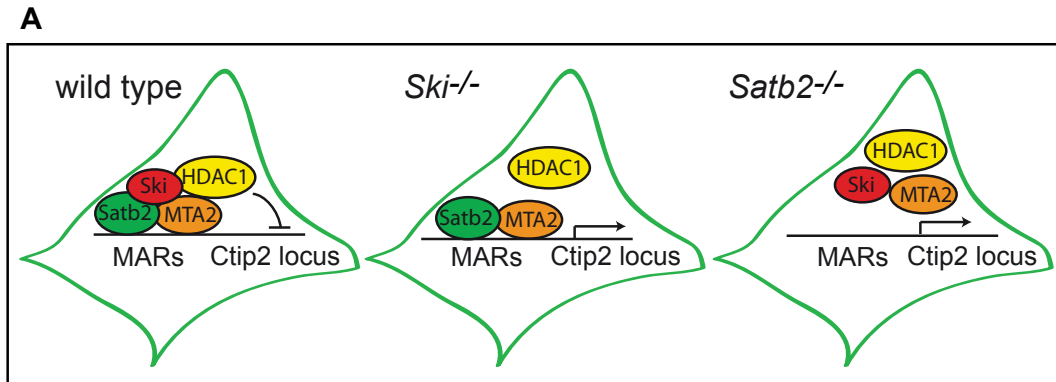


Fig.3.14. Model for Ski function at the *Ctip2* locus in callosal projection neurons.

Ski is required to assemble a functional NURD repressor complex containing Satb2, MTA2, and HDAC1 at MAR sites in the *Ctip2* locus. In the absence of Ski, Satb2 still binds the regulatory DNA sequences together with MTA2, but recruitment of HDAC1 is impaired. In the absence of Satb2, the NURD complex is not assembled. Thus, Satb2 and Ski play specific roles in the formation of a functional NURD complex, and individual loss of these factors prevents transcriptional repression of *Ctip2* in callosal projection neurons.

4 Discussion

Great progress has been made in recent years in identifying numerous subtype specific genes in the cortical plate. However, in most cases their function remains unclear and very few regulatory molecular mechanisms have been described yet. In this work we identify the transcriptional regulator Ski as a new factor in callosal neurons specification by cooperating with Satb2 in these cells.

4.2 Spatio-temporal expression pattern of Ski

All former studies of the expression pattern of Ski, whether in the developing embryo or postnatal brain, were done by *in situ* hybridisation (Lyons et al., 1994; Leferovich et al., 1995). It has been shown that Ski transcripts are highly expressed in germinal layers and in the cortical plate (Lyons et al., 1994). Since various genes are posttranscriptionally regulated, we determined the spatio-temporal expression pattern of the Ski protein. Our findings are more precise than the *in situ* data since we are able to identify for the first time the specific cell types in which the Ski protein is actually expressed, and thus where Ski might perform its function in the developing brain.

Our detailed analysis of co-expressed markers revealed an expression of Ski in specific subtypes of progenitor cells as well as in post-mitotic projection neurons. Ski was found to be expressed in apical progenitor cells together with the neural stem cell and radial glia marker Sox2 and Pax6. As soon as the cortical plate is established Ski expression also appears in post-mitotic neurons of this compartment. Notably, no Ski expression was found in Tbr2 positive IPCs of the SVZ.

Similar expression patterns have been previously described for the marker OTX1 and Fezf2 – both have been shown to be expressed in VZ precursor cells, down regulated in SVZ precursor cells and again up regulated in specific deep-layer neurons. Interestingly, both OTX1 and Fezf2 have a crucial role in specifying axonal projections in subsets of deep layer neurons (Weimann et al., 1999; Hirata et al., 2004; Molyneaux et al., 2005). However,

it is still not clear if the expression of a factor in the VZ correlates with the specification of the neuronal subpopulations or if these genes have two independent functions in different compartments (Alvarez-Bolado et al., 1995).

4.3 Does Ski function independently in different compartments?

The expression of Ski in both proliferative VZ progenitors and postmitotic neurons raises the question if Ski acts independently in different compartments. Ski has already been shown to promote differentiation in muscles and Schwann cells and also to be involved in cancerogenesis as either tumor suppressor or oncogene (Sutrave et al., 1990; Atanasoski et al., 2004; Pardali and Moustakas, 2007). This indicates defined roles in both proliferation as well as in differentiation. Furthermore, the interaction of Ski with the retinoblastoma protein (pRb) might be a direct link between Ski and the regulation of the cell cycle machinery in apical progenitor cells as well as its co-localisation with the centrosomes and the mitotic spindle during mitosis (Tokitou et al., 1999; Marcelain and Hayman, 2005). Our present finding, that in the absence of Ski the VZ of the dorsal telencephalon is thinner and fewer cells are in M-phase, accompanied by precocious differentiation due to a defect in proliferation and an exhaustion of the progenitor pool, is consistent with this proposition.

4.4 The Role of Ski in intermediate progenitors and migration

Surprisingly, the amount of cells in the cortical layers at perinatal stage was comparable to that in wild-type littermates with a somewhat higher density due to overall reduced body size of the knock-out animal as reported before (Berk et al., 1997). This is an unexpected result, considering the previously described effects of premature differentiation and proliferation defects. Birth-dating analysis revealed that in fact less neurons were born at early stages

(E10.5 and E12.5), consistent with the defect in apical progenitors proliferation, which are the main source for neurons at these stages. On the contrary, the amount of late born (E14.5) neurons was increased – due to increased proliferation of intermediate progenitor cells of the SVZ. This finding helps to explain how the initial defect in neuronal number could have been compensated. Still puzzling about this finding is that Ski itself is not expressed in intermediate progenitors and also that the amount of Tbr2 positive cells at early stage was reduced. It is still not clear which mechanisms regulate intermediate progenitor proliferation. By showing that intermediate progenitor cell proliferation changes during cortical development, Kowalczyk et al. supports the idea of a dynamic regulated system (Kowalczyk et al., 2009). Several factors that may selectively regulate intermediate progenitor cell proliferation were identified in recent years, such as Id4 (Yun et al., 2004) , delta notch signalling (Mizutani et al., 2007), secreted morphogens such as Wnts (Zhou et al., 2006), beta-catenin signalling (Mutch et al., 2010) and also the cell cycle protein CyclinD2 (Glickstein et al., 2009).

In the case of Ski deficiency, further investigations will be needed to elucidate if here an intrinsic effect in apical progenitors is influencing daughter cell types, since intermediate progenitor cells are produced by apical progenitors, or if an extrinsic effect of cell signalling cascades signal the need for increased cell production.

The same is true for the role of Ski in migration. It is not clear which mechanism causes the effects we see. Since migration of early born neurons (E10.5-12.5) appeared normal, the main differences were found in late born neurons born at E14.5. Beside the expected and normal migrating population of the upper layers neurons, the cells produced in excess, migrate to balance the deficit in the deep layers. Nevertheless the layering of the CP remained unaffected since Cux1 positive upper layers and also Tbr1 positive deep-layers emerged normally.

4.5 Ski interacts with Satb2 in a transcriptional complex

Although the layering of the cortex and expression of upper-layer markers appeared normal, we found ectopic expression of Ctip2 in upper layer neurons. Birth-dating analysis revealed that these cells were born at the expected time-point. This raised the question whether the genetic program of these cortical projection neurons was disturbed.

In *Satb2* deficient mice, a comparable phenotype has been described in the case of increased Ctip2 expression in upper-layer neurons (Alcamo et al., 2008; Britanova et al., 2008a). However, the effects were not completely identical in both knock-outs. Some neurons in *Satb2* mutants exhibit a delayed migration, which we could not find in our *Ski* deficient mice. Also, a comparison of gene expression data by *in situ* analysis between our present results in *Ski* deficient mice and the published results of Alcamo et al in *Satb2* knock-out mice revealed only partially corresponding effects (Alcamo et al., 2008). For example, CSMN specific genes such as *Clim1/Ldb2* and *Cdh13* displayed increased expression levels in both *Ski* and *Satb2* knock-out animals. On the other hand, interestingly, CPN specific genes such as *Cdh10*, *Ptn* and *Lmo4* were up-regulated upon loss of *Ski* in opposition to the observed effects in *Satb2* deficient mice. Nevertheless, overall the comparable phenotype of *Ski*^{-/-} and *Satb2*^{-/-} mice in respect to Ctip2 expression suggests that the function of *Ski* and *Satb2* is closely related in upper-layers where these two proteins are mainly co-expressed.

Our findings show that *Ski* interacts with *Satb2* in a transcriptional complex, which regulates Ctip2 expression in upper-layer neurons. *Satb2* as well as its family member *Satb1* is known to function either as a transcriptional activator or repressor by binding to MAR sites (Britanova et al., 2005). It is also known that *Satb2* represses Ctip2 transcription by recruiting the NURD complex, that contains amongst other factors two histone deacetylases, MTA2 and HDAC1 (Britanova et al., 2008a). This complex fails to function if either *Ski* or *Satb2* is absent. Alcamo et al identified several binding sites in the promoter of Ctip2 and they were able to show that *Satb2* interacts differently with each of these regions (Alcamo et al., 2008). In *Ski* deficient mice, the binding of *Satb2* to

these regions is not impaired, but we provide evidence that Ski is essential for recruiting HDAC1 and assure a correct complex formation.

4.6 Ski binds with Satb2 to specific regulatory regions of *Ctip2* in cortical neurons

In differentiated Satb2-deficient neural stem cells, it has been shown that there is preferential H3K4 dimethylation at MAR site A4. This shows that the chromatin at this site is transcriptionally active in the absence of Satb2 (Alcamo et al., 2008). Consistent with this finding, we were able to show with ChIP experiments that binding of Ski is strongest to the A4 site in wt cortical tissue. The binding of Ski to the other identified Satb2-binding sites (amplicons A1-A3, A5, A6) was weaker or not detectable. The result shows that not all MAR sites within the *Ctip2* locus are equally targeted by Ski in UL neurons. This proposition is also supported by the results obtained from cultured neural stem cells upon forced Satb2 expression {Alcamo:2008cc}.

4.7 Does Ski act cell autonomously in callosal projection neurons?

Ski and Satb2 are both co-expressed in cortical neurons that extend axons to the corpus callosum. In both the Satb2 knock-out mice and in the Ski deficient mice, the corpus callosum is severely reduced or even absent due to a redirection of the callosal projections subcortically through the cerebral peduncle (Alcamo et al., 2008). We find here that the callosal structures, including the glial sling and the glial wedge, are intact in Ski deficient mice. This argues strongly for a cell autonomous interaction of Ski and Satb2 in callosal projection neurons and rather excludes the possibility of a dorsal midline defect in this region.

It is known that subcortical and corticocortical projection neurons can coexist within a layer (Fame et al., 2011). In deep-layers, the percentage of Ski-Satb2 double positive cells is lower, and ectopic expression of *Ctip2* in these cell

populations is less obvious in the absence of Ski. It is also known that Satb2-expressing deep-layer neurons consist of a heterogeneous population of projecting neurons (Britanova et al., 2008a). Therefore Ski might be selectively expressed in Satb2 positive callosal projecting deep-layer neurons.

Since Ski expression appears preferentially in younger neurons, a second alternative explanation is that Ski could act here transiently in late born neurons to initiate proper callosal neuron identity. In support of this hypothesis we show here for the first time an interaction of Ski with the NURD complex, one of the two major histone deacetylation complexes, the other being the Sin3 complex. In several studies it has been shown that the NURD complex is particularly important for developmental transitions and lineage choice. The Sin3 complex appears instead to be in the control of cell cycle progression, proliferation and differentiation (for review see (McDonel et al., 2009)). The interaction of Ski with Sin3A has already been shown (Nomura et al., 1999). Reviewing our results in this context leads to the suggestion that Ski might play a fundamental role in development by interacting with both. Therefore the early defects could be due to a Sin3A defect in neural progenitors and the non-functional NURD complex could cause the later defects. A function for Ski together with the NURD complex in defining lineage choice would also explain the higher percentage of Ski-Satb2 double positive cells in later born upper-layers.

The only partially overlapping phenotypes of gene expressions in the cortical plate between Ski and Satb2 deficient mice could be explained by the fact that Ski and Satb2 have different spatio-temporal expression patterns and are only mainly coexpressed in UL-neurons, whereas in DL neurons they are not always co-expressed. It can be expected that they play different roles and have different impact in cells in which they are not co-expressed.

4.8 Concluding remarks

In summary, we demonstrate that Ski function in *Satb2*-expressing callosal neurons is essential to maintain their identity, and that the presence of both transcriptional regulators is required for repressing the genetic program of subcortically projecting neurons.

Still, many questions remain for prospective studies about the role of Ski in cortical development. What role does Ski play in apical progenitors? How does Ski deficiency influence basal progenitor proliferation? Which mechanism allows late born neurons to fill up missing deep layer populations? If Ski plays a role in cell identity determination, does this also apply for other cell types in the brain such as glia cells?

Altered proportion in cleavage plane distribution and misregulation of specific genes linked with asymmetric divisions in Ski deficient mice (preliminary data) might be a starting-point to explain the early effects we reported. *Lmo4*, a transcription factor up regulated in the CP of Ski deficient mice at E17.5 but down regulated in *Satb2* knock-out mice, is also a specific intermediate progenitor marker at earlier time-points (Sessa et al., 2008). Microarray analysis at E14.5 in Ski deficient animals has already revealed increased amounts of *Lmo4* transcripts at 14.5 (data not shown), suggesting that Ski might play a role in the specific regulation of this factor. Alfano et al. have shown that COUP-TFI promotes radial migration by repression of *Rnd2* (Alfano et al., 2011). Altered levels of COUP-TFI in Ski deficient mice (preliminary data) suggest that misregulation of COUP-TFI might lead to the reported migration defects in ski knock-out mice. Finally, expression studies in spinal cord of Ski knock-out mice revealed altered expression of GFAP positive cells (preliminary data). Together with the newly reported interaction with the NURD complex shown here, the reported need of DNA methylation of the GFAP gene promoter for enabling CNS stem cells to differentiate into astrocytes supports the hypothesis of a role of Ski in cell identity determination (Okano and Temple, 2009).

Further studies with conditional Ski knock-out mice will be needed to solve these questions.

5 Material and Methods

5.2 Mice

All mouse studies were approved by the veterinary office of the Canton of Basel Stadt and were performed in accordance with Swiss law. Ski mutant mice were generated and genotyped as described previously (Berk et al., 1997), and were maintained on a pure C57BL/6 background (Colmenares et al., 2002). We have used C57BL6/J congenics, since mutant fetuses in the 129 genetic background suffer from exencephaly and show gradually degenerating brain tissue during embryonic development (Berk et al., 1997). We intercrossed *Ski*^{+/-} mice to obtain *Ski*^{-/-} and control *Ski*^{+/+} littermates, and considered the day of vaginal plug as E0.5. *Satb2*^{-/-} P0 pups were provided by V. Tarabykin (Britanova et al., 2008b)

5.3 Immunohistochemistry, microscopy and image analysis

Embryos were fixed with 4% paraformaldehyde (wt/vol), cryoprotected with 30% sucrose (wt/vol) overnight, and embedded in OTC (Leica, Germany). 12µm horizontal (E10.5) and coronal (E12.5 to E17.5) sections were processed (Microm HM560) for immunohistochemistry.

For immunohistochemistry, antigen retrieval was performed by incubating sections in a pressure cooker in Citrate Buffer (pH 6) for 10 min at 100 C, blocked and incubated 4h to overnight at room temperature. For BrdU detection sections were additional treated with 2N HCl at 37C for 15min, neutralized in 0,1M borat buffer (pH 8,5) and washed in PBS.

We used following primary antibodies:

goat	Sox2	1:200	SantaCruz Biotechnology
rat	L1	1:50	Chemicon
rat	BrdU	1:100	Novus Biologicals
rabbit	Ski	1:200	SantaCruz Biotechnology
rabbit	Tbr1	1:200	Abcam
rabbit	Tbr2	1:200	Abcam
rabbit	Ctip2	1:400	Novus Biologicals
rabbit	Dcx	1:200	Cell-Signaling Tech
rabbit	GFAP	1:200	Dako
rabbit	pHH3	1:200	Upstate Biotechnology
rabbit	MTA2	1:300	Abcam
rabbit	HDAC1	1:200	Millipore
mouse	Satb2	1:50	Abcam
mouse	Pax6	1:100	DSHB
mouse	HuC/D	1:50	Invitrogen
mouse	NeuN	1:200	Chemicon
mouse	MTA2	1:300	Abcam

Where necessary, signal amplification was achieved using the TSA Plus System from PerkinElmer according to the manufacturer's instructions.

Secondary antibodies

Cy2	Goat-anti rat	1:100	Jackson Laboratories
Cy3	Goat-anti-rabbit	1:200	Jackson Laboratories
Cy5	Donkey-anti- mouse	1:100	Jackson Laboratories
Alexa488	Goat-anti-mouse	1:200	Molecular Probes
Alexa488	Goat-anti-rabbit	1:200	Molecular Probes

All cryosections were counterstained with DAPI or ToPro (Invitrogen).

Tissue sections were viewed on a Zeiss Image Z1 microscope equipped with an X-Cite 120 illuminator (EXFO), and images were collected and analyzed with Axio Vision Image Analysis Software (Improvision, 4.8.1). Alternatively, images were procured on a Zeiss LSM 510 Meta Axiovert 100M confocal microscope. Images were optimized for size, color, and contrast using Photoshop CS4 (Adobe).

5.4 BrdU Birthdating

Timed pregnant females received a single intraperitoneal injection of BrdU (40 mg/kg of body weight) at E10.5, E12.5 or E14.5. Pups were collected at E17.5 and processed for BrdU immunohistochemistry. At least three sets of wt and *Ski*^{-/-} littermates were examined for each time point. Quantification of BrdU-labeled cells and distribution within cortical layers were analysed. We selected a minimum of 3 anatomically matched sections from each mouse, and fluorescence photomicrographs were obtained spanning the motor cortex. The cortical plate was divided evenly into ten bins, and the distribution of

strongly BrdU-positive cells in all bins was determined in a 500- μ m-wide column. The paired t-test was used for statistical analysis.

5.5 *In situ* hybridization on tissue sections

Non-radioactive *in situ* hybridizations were performed according to a modified protocol by D. Henrique (IRFDBU, Oxford, UK). Cryosections were brought to room temperature, and hybridization buffer supplemented with DIG-labeled cRNA treated for 10 min at 95°C was added. Hybridization was performed overnight at 68°C in buffer containing 50% formamide (v/v), 10% dextran sulfate (w/v), 1 mg/ml yeast RNA, 1× Denhardt's, 5 mM EDTA, 12.6 mM Tris-HCl, pH 7.5, 185 mM NaCl, 5 mM Na₂HPO₄, 0.5 mM NaH₂PO₄. On the following day, slides were washed 1h at 65°C in 1× SSC, 50% formamid, 0.1% Tween 20, and 2x 1h at room temperature in 100 mM maleic acid, 150 mM NaCl adjusted to pH 7.5, supplemented with 0.1% Tween 20 (MABT). Sections were blocked 1h with MABT supplemented with 0,5% BSA (Sigma Aldrich) (MABT/BSA) before incubation in anti-DIG alkaline phosphatase conjugate (Roche, Mannheim, Germany) in MABT/BSA (1:5000) at room temperature overnight. On the following day, slides were washed for 1h in MABT and 2×10 min in alkaline phosphatase buffer (AP-Buffer) containing 100 mM Tris-HCl, pH 9.5, 50 mM MgCl₂, 100 mM NaCl, 0.24 mg/ml levamisole, 0.1% Tween 20. The color reaction was started by adding Deep Purple AP-substrate 1:1 in AP-Buffer (Roche, Mannheim, Germany). The reaction was performed in the dark at room temperature for several hours and stopped by washing in phosphate-buffered saline (PBS). After washing, sections were mounted in Kaiser's Glycerin-gelatine (Merck, Darmstadt, Germany).

5.6 Preparation of *in situ* hybridization probes

cDNAs were prepared from total E17.5 wt mouse brain RNAs using the SuperScript II Reverse Transcriptase (RT) (Invitrogen, Switzerland) according to the manufacturer's instructions. 1.5 µl of cDNA from the RT reaction was then amplified by PCR in the presence of 10 pM primer, with the negative strand primer additionally containing a promoter for T7 RNA polymerase. PCR products were then purified using the QIAquick PCR Purification Kit according to the manufacturer's instructions. The expected sizes of the probe products were checked by electrophoresis on a 1% agarose gel and the probes were quantified using a Nanodrop spectrophotometer (Thermo Scientific, Switzerland). 300ng of the DNA probes were transcribed using digoxigenin-UTP (DIG-UTP, Roche, Switzerland) by *in vitro* transcription with T7 RNA polymerase (Roche, Switzerland) at 37°C for 2h. The DIG-labeled riboprobes were then purified using the RNeasy kit (Qiagen, Switzerland) according to the manufacturer's instructions. The amount of DIG-labeled riboprobes was determined using a Nanodrop spectrophotometer (Thermo Scientific, Switzerland). The sequences of primers used are listed in pairs below, with the forward primer listed first. All reverse primers had the T7 promoter sequence (5'-GCGCGTAATACGACTCACTATAGGGC-3') added to their 5' end.

Bcl6: 5'-CATCATGGCCTACCGAGG-3'
 5'-CCCACTGGCACTGAGCTT-3'

Bhlhb5: 5'-CAGCCTCTCTTCCCAGCTCC-3'
 5'-CTGTA CTT CCTTGAGATCTAG-3'

Cdh10: 5'-AAAAAGCTCCGGCGAGAT-3'
 5'-CAGGCTGCATATCACACCA-3'

Cdh13: 5'-GAATGCCACAGACCCAGACT-3'
 5'-CTTGGGAGTCAAGCTTCAGG-3'

Ctip2: 5'-GCTGCGGCTCTGGCGGATGA-3'

	5'-GACGATGTGGCGAAAGGC-3'
Cux1:	5'-AAGAAGGCTGCGAACTTGAA-3'
	5'-CCCCCTTCCTGGTTTAAGAA-3'
Cux2:	5'-AGACAGGGCTCTGGTGAAGA-3'
	5'-AAGGTGACCTCTGGGGCTAT-3'
DKK3:	5'-ACGGCTGAAGCAATGAACTT-3'
	5'-GATGCGATTTACAGGCGTTT-3'
Fezf2:	5'-CAGCTTCCCTGGAGACCA-3'
	5'-ACACCTTGCCGCACACTT-3'
Lmo4:	5'-AGAATTGCTCATCCCAGGTG-3'
	5'-TTCATTCAGCAAATTAGAAGTAGGG-3'
Ptn	5'-GACTGTGGATTGGGCACC-3'
	5'-CATCGTTGCTCTGCCTCTC-3'
ROR β	5'-GTGTACAGCAGCAGCATTAGCA-3'
	5'-GGTCTCATCATCCAGGTGCTTC-3'

5.7 Axonal tracing

After fixation of the brains in 4% PFA, single crystals of 1,1'-dioctadecyl-3,3,3',3'-tetramethylindocarbocyanine perchlorate ('Dil'; DiI18(3), Molecular Probes) were placed in E18.5 cortices just lateral to the midline from rostral to caudal of one hemisphere to label callosal axons. Dil crystals were placed in the cerebral peduncle to study the distribution of subcortically projecting neurons in the cortex. At least three mice were used per genotype. Brains were stored in the dark at room temperature for at least 4 weeks to allow Dil diffusion. Brains were embedded in 2% agarose and cut at 100 μ m on a Vibratome (Microm HM 650V). The coronal sections were counterstained with DAPI and mounted with Vectamount (Vector Laboratories). Digital images were taken using an AxioCam camera (Zeiss). Alternatively, brains were transected coronally, rostral to the superior colliculus, to gain access to the

cerebral peduncle. Post injection, the brains were incubated for two weeks in the dark at 37°C. Thereafter, the brains were sectioned into 60µm thick sections using a Leica vibroslicer. The sections were stained with an antibody against Satb2. Images were procured on an inverted Leica confocal microscope (TCS-SP2 AOBS), at a pinhole of 1AU. Overview images were procured on a Zeiss microscope. The proportion of subcortically projecting cells that were Satb2 positive was counted manually. Statistical analysis was done using R and the two-tailed students t-test was used to determine statistical significance.

5.8 Transient transfection of HEK cells

HEK293T cells were grown in DMEM (4,5 gluc./l; Invitrogen) containing 10% FCS. Cells were transfected with Ski (Atanasoski et al., 2004) and Satb2 expression plasmids using JetPEI transfection reagent (Polyplus transfection) according to the manufacturer's recommendations. Cell lysates were prepared in a buffer containing 50 mM Tris-HCl [pH 7.5], 150 mM NaCl, 1% Triton X-100, and MiniComplete Protease inhibitors (Roche). After clearing by centrifugation (1000 x g, 5 min), supernatants were subjected to immunoprecipitation and immunoblotting.

5.9 Chromatin immunoprecipitation (ChIP), coimmunoprecipitation (co-IP), and immunoblotting

The ChIP assay was performed using the EZ-ChIP Kit (Upstate Biotechnology) according to the manufacturer's instructions. Cortices from E18.5 embryos or P0 pups were used for crosslinking of proteins and sonication of DNA as described. *Ctip2* locus primer sequences (A1 to A6) are as described previously and control GAPDH primer sequences are as described. For the co-IPs we used lysates of cortices from E18.5 embryos or cell lysates, and processed them using the Dynabeads Protein G Immunoprecipitation kit (Invitrogen) according to the manufacturer's instructions. Immunoprecipitations were carried out overnight at 4°C with 5-10

µg of the following antibodies: rabbit anti-Ski (Santa Cruz Biotechnology), rabbit anti-MTA2 (Abcam), rabbit anti-HDAC1 (Millipore), mouse anti-Satb2 (Abcam), normal rabbit/mouse serum as negative control, and mouse anti-RNA polymerase (provided in the EZ-ChIP Kit, Upstate Biotechnology) as positive control. Proteins were identified by immunoblotting with mouse anti-Satb2 (1:50, Abcam), rabbit anti-Ski (1:5000, Santa Cruz Biotechnology), or goat anti-Ski (1:2000, Santa Cruz Biotechnology). Secondary antibodies were goat anti-mouse-AP (1:50 000; Santa Cruz Biotechnology), goat anti-rabbit-HRP (1:50 000, Santa Cruz Biotechnology), or bovine anti-goat-AP (1:50 000, Santa Cruz Biotechnology). ECL Western blotting Analysis System (GE Healthcare) or CDP-Star ready-to-use kit (Roche) was used for detection (Amersham).

5.10 Proximity ligation assay (PLA)

The principle of the technology is based on two unique bi-functional probes called PLA probes. Each PLA probe consists of a secondary antibody attached to a unique synthetic oligonucleotide, which acts as a reporter. The two species-specific secondary antibodies recognize the primary antibodies directed against the molecules of interest. If the primary antibodies are in close proximity (< 40nm distance), unique synthetic oligonucleotides attached to the secondary antibodies guide the formation of circular DNA strands. The DNA circles in turn served as templates for localized rolling-circle amplification, whose product is detected through hybridization of complementary fluorescence-labeled oligonucleotides (Söderberg et al., 2006). PLA was performed using the Duolink Kit II (Olink Bioscience) according to the manufacturer's instructions. Primary antibodies were used at the same dilutions as for immunohistochemistry. Secondary antibodies were anti-rabbit plus (Duolink II, Bioscience) and anti-mouse minus (Duolink II, Bioscience). All cryosections were counterstained with TO-PRO®-3 stain (Invitrogen).

5.11 Luciferase Assay

COS cells were cultured in DMEM with 4,5 g/l glucose (Invitrogen) and 10% FCS (Invitrogen). The expression plasmid Satb2 was constructed by PCR techniques using proofreading polymerase Tersus (Evrogen). The fragment was digested by AgeI and Xho I and cloned into the pC1 vector (Evrogen). The construct was verified by DNA sequencing. Cells were transfected with 100 ng of pfosluc vector containing amplicon A4 (3) (kindly provided by R. Grosschedl) and were cotransfected with 50 ng Satb2 and/or 200 ng Ski (1) plasmid as indicated. DNA amounts were adjusted to equal levels with pcDNA3. Luciferase assays were performed in 96-well plates using the Dual-Luciferase kit (Promega), and transfected cells were analyzed after 24 hr using a Lumat LB96V reader (BertholdTechnologies). All experiments were repeated at least three times with a minimum of twelve replicates for each data point.

5.12 Data analysis

Radial thickness of the neuroepithelium was quantified on anatomically matched forebrain sections using Axio Vision Image Analysis Software (Improvision, 4.8.1). We carried out all cell quantifications in the medio-lateral extent of the rostral cortex and counted cells in a 250- μ m-wide column through the cortical plate. For all quantifications, we analyzed at least three embryos per genotype and at least 2 sections per embryo. We determined statistical significance using Student's t-test.

6 References

- Akiyoshi, S., Inoue, H., Hanai, J., Kusanagi, K., Nemoto, N., Miyazono, K. and Kawabata, M.** (1999). c-Ski acts as a transcriptional co-repressor in transforming growth factor-beta signaling through interaction with smads. *J Biol Chem* **274**, 35269–35277.
- Alcamo, E. A., Chirivella, L., Dautzenberg, M., Dobрева, G., Fariñas, I., Grosschedl, R. and McConnell, S. K.** (2008). Satb2 Regulates Callosal Projection Neuron Identity in the Developing Cerebral Cortex. *Neuron* **57**, 364–377.
- Alfano, C., Viola, L., Heng, J. I.-T., Pirozzi, M., Clarkson, M., Flore, G., De Maio, A., Schedl, A., Guillemot, F. and Studer, M.** (2011). COUP-TFI promotes radial migration and proper morphology of callosal projection neurons by repressing Rnd2 expression. *Development* **138**, 4685–4697.
- Alvarez-Bolado, G., Rosenfeld, M. G. and Swanson, L. W.** (1995). Model of forebrain regionalization based on spatiotemporal patterns of POU-III homeobox gene expression, birthdates, and morphological features. *J. Comp. Neurol.* **355**, 237–295.
- Amaravadi, L. S., Neff, A. W., Sleeman, J. P. and Smith, R. C.** (1997). Autonomous neural axis formation by ectopic expression of the protooncogene c-ski. *Developmental Biology* **192**, 392–404.
- Arlotta, P., Molyneaux, B. J., Chen, J., Inoue, J., Kominami, R. and Macklis, J. D.** (2005). Neuronal Subtype-Specific Genes that Control Corticospinal Motor Neuron Development In Vivo. *Neuron* **45**, 207–221.
- Atanasoski, S., Notterpek, L., Lee, H.-Y., Castagner, F., Young, P., Ehrengruber, M. U., Meijer, D., Sommer, L., Stavnezer, E., Colmenares, C., et al.** (2004). The Protooncogene Ski Controls Schwann Cell Proliferation and Myelination. *Neuron* **43**, 499–511.
- Barrio, R., López-Varea, A., Casado, M. and de Celis, J. F.** (2007). Characterization of dSnoN and its relationship to Decapentaplegic signaling in Drosophila. *Developmental Biology* **306**, 66–81.

- Bedogni, F., Hodge, R. D., Elsen, G. E., Nelson, B. R., Daza, R. A. M., Beyer, R. P., Bammler, T. K., Rubenstein, J. L. R. and Hevner, R. F.** (2010). Tbr1 regulates regional and laminar identity of postmitotic neurons in developing neocortex. In *Proceedings of the National Academy of Sciences*, pp. 13129–13134.
- Berk, M., Desai, S. Y., Heyman, H. C. and Colmenares, C.** (1997). Mice lacking the ski proto-oncogene have defects in neurulation, craniofacial, patterning, and skeletal muscle development. *Genes & Development* **11**, 2029–2039.
- Bonnon, C. and Atanasoski, S.** (2012). c-Ski in health and disease. *Cell Tissue Res.* **347**, 51–64.
- Britanova, O., Akopov, S., Lukyanov, S., Gruss, P. and Tarabykin, V.** (2005). Novel transcription factor Satb2 interacts with matrix attachment region DNA elements in a tissue-specific manner and demonstrates cell-type-dependent expression in the developing mouse CNS. *European Journal of Neuroscience* **21**, 658–668.
- Britanova, O., Alifragis, P., Junek, S., Jones, K., Gruss, P. and Tarabykin, V.** (2006). A novel mode of tangential migration of cortical projection neurons. *Developmental Biology* **298**, 299–311.
- Britanova, O., de Juan Romero, C., Cheung, A., Kwan, K. Y., Schwark, M., Gyorgy, A., Vogel, T., Akopov, S., Mitkovski, M., Agoston, D., et al.** (2008a). Satb2 Is a Postmitotic Determinant for Upper-Layer Neuron Specification in the Neocortex. *Neuron* **57**, 378–392.
- Britanova, O., de Juan Romero, C., Cheung, A., Kwan, K. Y., Schwark, M., Gyorgy, A., Vogel, T., Akopov, S., Mitkovski, M., Agoston, D., et al.** (2008b). Satb2 is a postmitotic determinant for upper-layer neuron specification in the neocortex. *Neuron* **57**, 378–392.
- Calegari, F. and Huttner, W. B.** (2003). An inhibition of cyclin-dependent kinases that lengthens, but does not arrest, neuroepithelial cell cycle induces premature neurogenesis. *Journal of Cell Science* **116**, 4947–4955.

- Cohen, S., Zheng, G., Heyman, H. and Stavnezer, E.** (1999). Heterodimers of the SnoN and Ski oncoproteins form preferentially over homodimers and are more potent transforming agents. *Nucleic Acids Research* **27**, 1006–1014.
- Colmenares, C. and Stavnezer, E.** (1995). Enhanced expression of mouse c-ski accompanies terminal skeletal muscle differentiation in vivo and in vitro - Namciu - 2005 - Developmental Dynamics - Wiley Online Library. *Developmental*
- Colmenares, C., Heilstedt, H. A., Shaffer, L. G., Schwartz, S., Berk, M., Murray, J. C. and Stavnezer, E.** (2002). Loss of the SKI proto-oncogene in individuals affected with 1p36 deletion syndrome is predicted by strain-dependent defects in Ski^{-/-} mice. *Nat Genet* **30**, 106–109.
- Cubelos, B., Sebastian-Serrano, A., Beccari, L., Calcagnotto, M. E., Cisneros, E., Kim, S., Dopazo, A., Alvarez-Dolado, M., Redondo, J. M., Bovolenta, P., et al.** (2010). Cux1 and Cux2 Regulate Dendritic Branching, Spine Morphology, and Synapses of the Upper Layer Neurons of the Cortex. *Neuron* **66**, 523–535.
- Dahl, R., Kieslinger, M., Beug, H. and Hayman, M. J.** (1998). Transformation of hematopoietic cells by the Ski oncoprotein involves repression of retinoic acid receptor signaling. *Proc Natl Acad Sci USA* **95**, 11187–11192.
- Dai, P., Shinagawa, T., Nomura, T., Harada, J., Kaul, S. C., Wadhwa, R., Khan, M. M., Akimaru, H., Sasaki, H., Colmenares, C., et al.** (2002). Ski is involved in transcriptional regulation by the repressor and full-length forms of Gli3. *Genes & Development* **16**, 2843–2848.
- Englund, C.** (2005). Pax6, Tbr2, and Tbr1 Are Expressed Sequentially by Radial Glia, Intermediate Progenitor Cells, and Postmitotic Neurons in Developing Neocortex. *Journal of Neuroscience* **25**, 247–251.
- Glickstein, S. B., Monaghan, J. A., Koeller, H. B., Jones, T. K. and Ross, M. E.** (2009). Cyclin D2 is critical for intermediate progenitor cell proliferation in the embryonic cortex. *Journal of Neuroscience* **29**, 9614–9624.

- Gotz, M. and Huttner, W. B.** (2005). The cell biology of neurogenesis. *Nat Rev Mol Cell Biol* **6**, 777–788.
- Gotz, M., Stoykova, A. and Gruss, P.** (1998). Pax6 controls radial glia differentiation in the cerebral cortex. *Neuron* **21**, 1031–1044.
- Haubensak, W., Attardo, A., Denk, W. and Huttner, W. B.** Neurons arise in the basal neuroepithelium of the early mammalian telencephalon: A major site of neurogenesis.
- Heyman, H. C. and Stavnezer, E.** (1994). A carboxyl-terminal region of the ski oncoprotein mediates homodimerization as well as heterodimerization with the related protein SnoN. *J Biol Chem* **269**, 26996–27003.
- Hirata, T., Suda, Y., Nakao, K., Narimatsu, M., Hirano, T. and Hibi, M.** (2004). Zinc finger gene-fzf-like functions in the formation of subplate neurons and thalamocortical axons. *Dev. Dyn.* **230**, 546–556.
- Huttner, W. B. and Brand, M.** (1997). Asymmetric division and polarity of neuroepithelial cells. *Current Opinion in Neurobiology* **7**, 29–39.
- Inoue, Y., Iemura, S.-I., Natsume, T., Miyazawa, K. and Imamura, T.** (2011). Suppression of p53 activity through the cooperative action of Ski and histone deacetylase SIRT1. *Journal of Biological Chemistry* **286**, 6311–6320.
- Karagianni, P. and Wong, J.** (2007). HDAC3: taking the SMRT-N-CoR road to repression. *Oncogene* **26**, 5439–5449.
- Kaufman, C. D., Martínez-Rodríguez, G. and Hackett, P. B.** (2000). Ectopic expression of c-ski disrupts gastrulation and neural patterning in zebrafish. *Mech Dev* **95**, 147–162.
- Kim, S.-S., Zhang, R.-G., Braunstein, S. E., Joachimiak, A., Cvekl, A. and Hegde, R. S.** (2002). Structure of the retinal determination protein Dachshund reveals a DNA binding motif. *Structure* **10**, 787–795.
- Kokura, K., Kaul, S. C., Wadhwa, R., Nomura, T., Khan, M. M., Shinagawa, T., Yasukawa, T., Colmenares, C. and Ishii, S.** (2001). The Ski protein family is required for MeCP2-mediated

- transcriptional repression. *J Biol Chem* **276**, 34115–34121.
- Kowalczyk, T., Pontious, A., Englund, C., Daza, R. A. M., Bedogni, F., Hodge, R., Attardo, A., Bell, C., Huttner, W. B. and Hevner, R. F.** (2009). Intermediate Neuronal Progenitors (Basal Progenitors) Produce Pyramidal-Projection Neurons for All Layers of Cerebral Cortex. *Cerebral Cortex* **19**, 2439–2450.
- Kriegstein, A., Noctor, S. and Martínez-Cerdeño, V.** (2006). Patterns of neural stem and progenitor cell division may underlie evolutionary cortical expansion. *Nat Rev Neurosci* **7**, 883–890.
- Kulkarni, A. B., Thyagarajan, T. and Letterio, J. J.** (2002). Function of cytokines within the TGF-beta superfamily as determined from transgenic and gene knockout studies in mice. *Curr. Mol. Med.* **2**, 303–327.
- Lai, T., Jabaudon, D., Molyneaux, B. J., Azim, E., Arlotta, P., Menezes, J. R. L. and Macklis, J. D.** (2008). SOX5 Controls the Sequential Generation of Distinct Corticofugal Neuron Subtypes. *Neuron* **57**, 232–247.
- Leferovich, J. M., Lana, D. P., Sutrave, P., Hughes, S. H. and Kelly, A. M.** (1995). Regulation of c-ski transgene expression in developing and mature mice. *J Neurosci* **15**, 596–603.
- Li, Y., Turck, C. M., Teumer, J. K. and Stavnezer, E.** (1986). Unique sequence, ski, in Sloan-Kettering avian retroviruses with properties of a new cell-derived oncogene. *J Virol* **57**, 1065–1072.
- Luo, K., Stroschein, S. L., Wang, W., Chen, D., Martens, E., Zhou, S. and Zhou, Q.** (1999). The Ski oncoprotein interacts with the Smad proteins to repress TGFbeta signaling. *Genes & Development* **13**, 2196–2206.
- Lyons, G. E., Micales, B. K., Herr, M. J., Horrigan, S. K., Namciu, S., Shardy, D. and Stavnezer, E.** (1994). Protooncogene c-ski is expressed in both proliferating and postmitotic neuronal populations. *Dev. Dyn.* **201**, 354–365.
- Malatesta, P., Appolloni, I. and Calzolari, F.** (2008). Radial glia and neural stem cells. *Cell Tissue Res.* **331**, 165–178.

- Marcelain, K. and Hayman, M. J.** (2005). The Ski oncoprotein is upregulated and localized at the centrosomes and mitotic spindle during mitosis. *Oncogene* **24**, 4321–4329.
- McConnell, S. K.** (1995). Constructing the cerebral cortex: neurogenesis and fate determination. *Neuron* **15**, 761–768.
- McDonel, P., Costello, I. and Hendrich, B.** (2009). Keeping things quiet: roles of NuRD and Sin3 co-repressor complexes during mammalian development. *The International Journal of Biochemistry & Cell Biology* **41**, 108–116.
- Miyata, T.** (2004). Asymmetric production of surface-dividing and non-surface-dividing cortical progenitor cells. *Development* **131**, 3133–3145.
- Mizutani, K.-I., Yoon, K., Dang, L., Tokunaga, A. and Gaiano, N.** (2007). Differential Notch signalling distinguishes neural stem cells from intermediate progenitors. *Nature* **449**, 351–355.
- Molnár, Z. and Cheung, A. F. P.** (2006). Towards the classification of subpopulations of layer V pyramidal projection neurons. *Neuroscience Research* **55**, 105–115.
- Molyneaux, B. J., Arlotta, P., Hirata, T., Hibi, M. and Macklis, J. D.** (2005). Fez1 Is Required for the Birth and Specification of Corticospinal Motor Neurons. *Neuron* **47**, 817–831.
- Molyneaux, B. J., Arlotta, P., Menezes, J. R. L. and Macklis, J. D.** (2007). Neuronal subtype specification in the cerebral cortex. *Nat Rev Neurosci* **8**, 427–437.
- Mutch, C. A., Schulte, J. D., Olson, E. and Chenn, A.** (2010). Beta-Catenin Signaling Negatively Regulates Intermediate Progenitor Population Numbers in the Developing Cortex. *PLoS ONE* **5**, e12376.
- Nagase, T., Nomura, N. and Ishii, S.** (1993). Complex formation between proteins encoded by the ski gene family. *J Biol Chem* **268**, 13710–13716.
- Nelson, S. B., Hempel, C. and Sugino, K.** (2006). Probing the transcriptome of neuronal cell types. *Current Opinion in Neurobiology* **16**, 571–576.

- Nieto, M., Monuki, E. S., Tang, H., Imitola, J., Haubst, N., Khoury, S. J., Cunningham, J., Gotz, M. and Walsh, C. A.** (2004). Expression of Cux-1 and Cux-2 in the subventricular zone and upper layers II-IV of the cerebral cortex. *J. Comp. Neurol.* **479**, 168–180.
- Noctor, S. C., Flint, A. C., Weissman, T. A., Dammerman, R. S. and Kriegstein, A. R.** (2001). Neurons derived from radial glial cells establish radial units in neocortex. *Nature* **409**, 714–720.
- Noctor, S. C., Martínez-Cerdeño, V., Ivic, L. and Kriegstein, A. R.** (2004). Cortical neurons arise in symmetric and asymmetric division zones and migrate through specific phases. *Nat Neurosci* **7**, 136–144.
- Nomura, N., Sasamoto, S., Ishii, S., Date, T., Matsui, M. and Ishizaki, R.** (1989). Isolation of human cDNA clones of ski and the ski-related gene, sno. *Nucleic Acids Research* **17**, 5489–5500.
- Nomura, T., Khan, M. M., Kaul, S. C., Dong, H. D., Wadhwa, R., Colmenares, C., Kohno, I. and Ishii, S.** (1999). Ski is a component of the histone deacetylase complex required for transcriptional repression by Mad and thyroid hormone receptor. *Genes & Development* **13**, 412–423.
- Okano, H. and Temple, S.** (2009). Cell types to order: temporal specification of CNS stem cells. *Current Opinion in Neurobiology* 1–8.
- Pardali, K. and Moustakas, A.** (2007). Actions of TGF-beta as tumor suppressor and pro-metastatic factor in human cancer. *Biochim Biophys Acta* **1775**, 21–62.
- Parnavelas, J. G. and Nadarajah, B.** (2001). Radial glial cells. are they really glia? *Neuron* **31**, 881–884.
- Pessah, M., Marais, J., Prunier, C., Ferrand, N., Lallemand, F., Mauviel, A. and Atfi, A.** (2002). c-Jun associates with the oncoprotein Ski and suppresses Smad2 transcriptional activity. *J Biol Chem* **277**, 29094–29100.
- Rakic, P.** (1995). A small step for the cell, a giant leap for mankind: a hypothesis of neocortical expansion during evolution. *Trends in Neurosciences* **18**, 383–388.

- Rakic, P.** (2003). Developmental and evolutionary adaptations of cortical radial glia. *Cereb Cortex* **13**, 541–549.
- Rosenfeld, J. A., Crolla, J. A., Tomkins, S., Bader, P., Morrow, B., Gorski, J., Troxell, R., Forster-Gibson, C., Cilliers, D., Hislop, R. G., et al.** (2010). Refinement of causative genes in monosomy 1p36 through clinical and molecular cytogenetic characterization of small interstitial deletions. *Am. J. Med. Genet. A* **152A**, 1951–1959.
- Sessa, A., Mao, C.-A., Hadjantonakis, A.-K., Klein, W. H. and Broccoli, V.** (2008). Tbr2 Directs Conversion of Radial Glia into Basal Precursors and Guides Neuronal Amplification by Indirect Neurogenesis in the Developing Neocortex. *Neuron* **60**, 56–69.
- Shu, T., Li, Y., Keller, A. and Richards, L. J.** (2003). The glial sling is a migratory population of developing neurons. *Development* **130**, 2929–2937.
- Sleeman, J. P. and Laskey, R. A.** (1993). Xenopus c-ski contains a novel coiled-coil protein domain, and is maternally expressed during development. *Oncogene* **8**, 67–77.
- Söderberg, O., Gullberg, M., Jarvius, M., Ridderstråle, K., Leuchowius, K.-J., Jarvius, J., Wester, K., Hydbring, P., Bahram, F., Larsson, L.-G., et al.** (2006). Direct observation of individual endogenous protein complexes in situ by proximity ligation. *Nat. Methods* **3**, 995–1000.
- Stavnezer, E., Barkas, A. E., Brennan, L. A., Brodeur, D. and Li, Y.** (1986). Transforming Sloan-Kettering viruses generated from the cloned v-ski oncogene by in vitro and in vivo recombinations. *J Virol* **57**, 1073–1083.
- Stavnezer, E., Brodeur, D. and Brennan, L. A.** (1989). The v-ski oncogene encodes a truncated set of c-ski coding exons with limited sequence and structural relatedness to v-myc. *Molecular and Cellular Biology* **9**, 4038–4045.
- Sun, Y., Liu, X., Eaton, E. N., Lane, W. S., Lodish, H. F. and Weinberg, R. A.** (1999). Interaction of the Ski oncoprotein with Smad3 regulates TGF-beta signaling. *Molecular Cell* **4**, 499–509.

- Sutrave, P., Kelly, A. M. and Hughes, S. H.** (1990). ski can cause selective growth of skeletal muscle in transgenic mice. *Genes & Development* **4**, 1462–1472.
- Tarabykin, V., Stoykova, A., Usman, N. and Gruss, P.** (2001). Cortical upper layer neurons derive from the subventricular zone as indicated by Svet1 gene expression. *Development* **128**, 1983–1993.
- Tarapore, P., Richmond, C., Zheng, G., Cohen, S. B., Kelder, B., Kopchick, J., Kruse, U., Sippel, A. E., Colmenares, C. and Stavnezer, E.** (1997). DNA binding and transcriptional activation by the Ski oncoprotein mediated by interaction with NFI. *Nucleic Acids Research* **25**, 3895–3903.
- Tokitou, F., Nomura, T., Khan, M. M., Kaul, S. C., Wadhwa, R., Yasukawa, T., Kohno, I. and Ishii, S.** (1999). Viral ski inhibits retinoblastoma protein (Rb)-mediated transcriptional repression in a dominant negative fashion. *J Biol Chem* **274**, 4485–4488.
- Ueki, N. and Hayman, M. J.** (2003). Signal-dependent N-CoR requirement for repression by the Ski oncoprotein. *J Biol Chem* **278**, 24858–24864.
- Ueki, N., Zhang, L. and Hayman, M. J.** (2004). Ski negatively regulates erythroid differentiation through its interaction with GATA1. *Molecular and Cellular Biology* **24**, 10118–10125.
- Ueki, N., Zhang, L., Hayman, M. J. and Haymann, M. J.** (2008). Ski can negatively regulates macrophage differentiation through its interaction with PU.1. *Oncogene* **27**, 300–307.
- Wang, W., Mariani, F. V., Harland, R. M. and Luo, K.** (2000). Ski represses bone morphogenic protein signaling in *Xenopus* and mammalian cells. *Proc Natl Acad Sci USA* **97**, 14394–14399.
- Weimann, J. M., Zhang, Y. A., Levin, M. E., Devine, W. P., Brûlet, P. and McConnell, S. K.** (1999). Cortical neurons require Otx1 for the refinement of exuberant axonal projections to subcortical targets. *Neuron* **24**, 819–831.
- Wilson, J. J., Malakhova, M., Zhang, R., Joachimiak, A. and Hegde, R. S.** (2004). Crystal structure of the dachshund homology domain of human SKI. *Structure* **12**, 785–792.

- Wu, J. W., Krawitz, A. R., Chai, J., Li, W., Zhang, F., Luo, K. and Shi, Y.** (2002). Structural mechanism of Smad4 recognition by the nuclear oncoprotein Ski: insights on Ski-mediated repression of TGF-beta signaling. *Cell* **111**, 357–367.
- Xu, W., Angelis, K., Danielpour, D., Haddad, M. M., Bischof, O., Campisi, J., Stavnezer, E. and Medrano, E. E.** (2000). Ski acts as a co-repressor with Smad2 and Smad3 to regulate the response to type beta transforming growth factor. *Proc Natl Acad Sci USA* **97**, 5924–5929.
- Yun, K., Mantani, A., Garel, S., Rubenstein, J. and Israel, M. A.** (2004). Id4 regulates neural progenitor proliferation and differentiation in vivo. *Development* **131**, 5441–5448.
- Zheng, G., Blumenthal, K. M., Ji, Y., Shardy, D. L., Cohen, S. B. and Stavnezer, E.** (1997). High affinity dimerization by Ski involves parallel pairing of a novel bipartite alpha-helical domain. *J Biol Chem* **272**, 31855–31864.
- Zhou, C. J., Borello, U., Rubenstein, J. L. R. and Pleasure, S. J.** (2006). Neuronal production and precursor proliferation defects in the neocortex of mice with loss of function in the canonical Wnt signaling pathway. *Neuroscience* **142**, 1119–1131.

7 Acknowledgements

First of all I would like to thank Suzana Atanasoski for the opportunity to do my PhD thesis at her laboratory, for her guidance, support, the inspiring discussions and the freedom to get lost in Pubmed inventing new theories.

Thank you to Yves Barde and Lukas Sommer for scientific advice, critical discussions and helpful comments.

Thank you to my colleagues for the encouragement, helpful comments, ideas and the great team spirit. I also would like to thank the members of the anatomical institute for the nice working atmosphere.

Thank you a lot to Ueli Schneider and Nicole Caviezel for their great work at the animal facility.

Special thanks to all my friends for being there in both good times and in bad times.

And finally and most importantly I would like to thank my wonderful family, my mother Sabine and my siblings Julia and Peter for their unquestioning support and love in all these years and in all circumstances.

8 Curriculum Vitae

Personal profile

Name: Constanze Baranek
Date of birth: 27. July 1978
Place of birth: Munich
Address: Sperrstrasse 103, 4057 Basel
Email: Constanze.Baranek@unibas.ch

Education:

11/06 – present: University of Basel (Switzerland);
PhD in neurobiology, Institut of
physiology, at the group of Prof. S.
Atanasoski.
10/01 – 04/05 Friedrich Alexander University,
Erlangen-Nuernberg, Diploma in
Biology.
Diploma thesis at the group of Prof.
M.Wegner.
04/99 – 09/01 Johannes Gutenberg University,
Mainz, Pre-Diploma in Biology.
06/98 A-level (German Abitur)

Internships

09/02 – 12/02 Internship at the University of
Queensland, Brisbane / Australia

Languages

German – native language
English – fluent
French – basic level

Publications:

Baranek, C., Dittrich, M., Parthasarathy, S., Bonnon, C. G., Britanova, O., Lanshakov, D., Boukhtouche, F., Sommer, J. E., Colmenares, C., Tarabykin, V., et al. (2012). Protooncogene Ski cooperates with the chromatin-remodeling factor Satb2 in specifying callosal neurons. *Proc Natl Acad Sci USA*.

Atanasoski, S., Boentert, M., De Ventura, L., Pohl, H., **Baranek, C.**, Beier, K., Young, P., Barbacid, M. and Suter, U. (2008). Postnatal Schwann cell proliferation but not myelination is strictly and uniquely dependent on cyclin-dependent kinase 4 (cdk4). *Mol Cell Neurosci* 37, 519–527

Baranek, C., Sock, E. and Wegner, M. (2005). The POU protein Oct-6 is a nucleocytoplasmic shuttling protein. *Nucleic Acids Research* 33, 6277–6286.

